University of Alberta

Assessment of Microalgal Atmospheric Carbon Dioxide Sequestration Systems

by

Glen Tichkowsky

A thesis submitted to the Faculty of Graduate Studies and Research
in partial fulfillment of the requirements for the degree of

Master of Science

Mechanical Engineering

Edmonton, Alberta
Spring 2008

Library and Archives Canada

Published Heritage Branch

395 Wellington Street
Ottawa ON K1A 0N4
Canada

Bibliothèque et Archives Canada

Direction du Patrimoine de l'édition

395, rue Wellington
Ottawa ON K1A 0N4
Canada

Your file Votre référence
ISBN: 978-0-494-45897-6
Our file Notre référence
ISBN: 978-0-494-45897-6

NOTICE:
The author has granted a non-exclusive license allowing Library and Archives Canada to reproduce, publish, archive, preserve, conserve, communicate to the public by telecommunication or on the Internet, loan, distribute and sell theses worldwide, for commercial or non-commercial purposes, in microform, paper, electronic and/or any other formats.

The author retains copyright ownership and moral rights in this thesis. Neither the thesis nor substantial extracts from it may be printed or otherwise reproduced without the author's permission.

AVIS:
L'auteur a accordé une licence non exclusive permettant à la Bibliothèque et Archives Canada de reproduire, publier, archiver, sauvegarder, conserver, transmettre au public par télécommunication ou par l'Internet, prêter, distribuer et vendre des thèses partout dans le monde, à des fins commerciales ou autres, sur support microforme, papier, électronique et/ou autres formats.

L'auteur conserve la propriété du droit d'auteur et des droits moraux qui protège cette thèse. Ni la thèse ni des extraits substantiels de celle-ci ne doivent être imprimés ou autrement reproduits sans son autorisation.

In compliance with the Canadian Privacy Act some supporting forms may have been removed from this thesis.

While these forms may be included in the document page count, their removal does not represent any loss of content from the thesis.

Conformément à la loi canadienne sur la protection de la vie privée, quelques formulaires secondaires ont été enlevés de cette thèse.

Bien que ces formulaires aient inclus dans la pagination, il n'y aura aucun contenu manquant.

Canada

Abstract

The objective of this thesis is to evaluate an atmospheric carbon dioxide sequestration system which uses microalgae, which perform photosynthesis, to capture carbon dioxide. The microalgae are sent to the deep ocean for long term storage where they would remain for between 300 and 1000 years. The system used to capture the carbon dioxide consists of large unmixed ponds which grow microalgae species *Dunaliella* located in Western Australia. The microalgae are disposed to the deep ocean through a pipeline connected to the shore or through a suspended vertical pipe connected to a ship or floating platform. The low diffusion of carbon dioxide form the atmosphere to the pond medium results in the cost per tonne of CO_2 sequestered being higher than that for capturing CO_2 from a coal fired power plant and injecting it into the deep ocean. Therefore this system is not economically feasible.

Acknowledgment

The author would like to express profound gratitude to his supervisor, Dr. Peter Flynn for all of his support, advice, and encouragement over the duration of completing this work and over the duration of his academic work as well. His constant guidance and motivation made the academic life of the author very enjoyable and fulfilling.

The author would like to thank his parents Ken and Betty, his sister Laura, and his brother Neil for all of their support and encouragement in completing his Master of Science degree.

Finally, the author would like to thank Ashley Grant for her constant support and encouragement in completing his degree and many other aspects of his life.

Table of Contents

Chapter	Title	Page No.
1	**Introduction**	
	1.1 Greenhouse Gas Emissions and Climate Change	1-3
	1.2 Objective of this Thesis	3-4
	1.3 Background	
	1.3.1 Microalgal Atmospheric Carbon Dioxide Capture and Storage	4-8
	1.3.2 Ocean Water Density and Temperature Variation	8-11
	1.3.3 Ocean Topography	11-13
	1.4 Organization of the Thesis	13
2	**Microalgal Atmospheric Carbon Dioxide Capture and Storage System Options**	
	2.1 Microalgal Species for Commercial Production	
	2.1.1 Overview	14-15
	2.1.2 *Chlorella*	15-16
	2.1.3 *Spirulina*	16-18
	2.1.4 *Dunaliella*	18-19
	2.1.5 Selection of Microalgae Species	19-20
	2.2 Systems for Commercial Production of Microalgae	
	2.2.1 Overview	20-21
	2.2.2 Unmixed Ponds	21-23
	2.2.3 Circular Ponds	23-24
	2.2.4 Raceway Ponds	24-25

Table of Contents (cont'd)

Chapter	Title	Page No.
	2.2.5 Stirred Tank Fermentors	25-26
	2.2.6 Photobioreactors	26-29
	2.2.7 Selection of Microalgae Production System	29-30
	2.3 Geographic Location for Microalgae Production	
	2.3.1 Geographic Factors	30-36
	2.3.2 Selection of Geographic Location	37-38
	2.4 Microalgal Carbon Dioxide Capture and Storage System Design Alternatives	
	2.4.1 Overview	38
	2.4.2 Ocean Based System	38-44
	2.4.3 Land Based System at Very Near Sea Level	44-47
	2.4.4 Land Based System above Sea Level	47-49
	2.4.5 Selection of Microalgal Carbon Dioxide Capture and Storage System Design	49-50
	2.5 Chapter Summary	50-51
3	**Deep Ocean Disposal**	
	3.1 Introduction	52-53
	3.2 Down Flow Pipe	
	3.2.1 Overview	53-54
	3.2.2 Pipeline	54

Table of Contents (cont'd)

Chapter	Title	Page No.
	3.2.3 Suspended Vertical Pipe	54-56
	3.3 Density Driven Flow	
	3.3.1 Overview	56-57
	3.3.2 Temperature, Salinity, and Density	57-59
	3.3.3 Ocean Density Profile and Density Gradient	59-62
	3.3.4 Hydrostatic Head	62-65
	3.3.5 Friction	65-66
	3.3.6 Pond Depth and Density	66-67
	3.4 Required Pond Water Density	
	3.4.1 Overview	67
	3.4.2 Density Calculations	68-72
	3.4.3 Density Calculation Results	72-74
	3.4.4 Density, Salinity and Pond Depth Relationship	74-76
4	**Limiting Factors**	
	4.1 Introduction	77
	4.2 Evaporation Rate	77
	4.3 Microalgal Growth Rate	78
	4.4 Available Carbon	
	4.4.1 Ocean Water Carbon and pH	78-79
	4.4.2 Carbon Flux	80-82
	4.4.3 Total Available Carbon	82

Table of Contents (cont'd)

Chapter	Title	Page No.
	4.5 Summary	82
5	**Feasibility of Microalgal Atmospheric Carbon Dioxide Capture and Storage Systems**	
	5.1 Economic Feasibility of the Total Discharge Disposal System	
	5.1.1 Pond Area Requirements	83-84
	5.1.2 Cost of the Microalgal Pond System using the Total Discharge Disposal System	84-85
	5.2 Economic Feasibility of the Microalgal Concentration Disposal System	
	5.2.1 Pond Area Requirements	85-87
	5.2.2 Cost of the Microalgal Pond System using the Microalgal Concentration Disposal System	87-88
	5.3 Summary	89
6	**Conclusion and Recommendations for Future Research**	
	6.1 Conclusion	90-91
	6.2 Recommendations for Future Research	91-92
	References	93-101
	Appendix A	102-104
	Appendix B	105-109
	Appendix C	110-114

List of Tables

Table No.	Description	Page No.
2.3.1	Mean monthly and annual weather statistics for 28.80°S, 114.70°E in Western Australia.	37
2.4.1	Annual cost per tonne of CO_2 sequestered based on the capital cost of an ocean based structure for three microalgal growth rates.	44
3.4.1	List of symbols used in Section 3.4.2.	68
3.4.2	Parameters used to calculated density for the pipeline disposal system.	73
3.4.3	Parameters used to calculated density for the suspended vertical pipe disposal system.	74
3.4.4	Time (in days) required to reach the target density based on daily net evaporation rates for the pipeline system and the suspended vertical pipe system. The daily net evaporation rates used are the minimum monthly (0.03 mm d^{-1}), annual average (5.5 mm d^{-1}), and maximum monthly (10.6 mm d^{-1}).	76

List of Figures

Figure No.	Description	Page No.
1.3.1	Generalized density depth profile of the ocean showing the mixed layer, the pycnocline zone, and the deep ocean.	10
1.3.2	The Ocean Conveyor Belt.	11
1.3.3	Generalized profile of the continental margin showing the continental shelf, slope and rise.	12
2.3.1	Net evaporation (mm per month) for the month of October in the Pacific Ocean.	32
2.3.2	Topographical map of the ocean floor.	34
2.3.3	Ocean floor profile of three locations a) western coast of South America, b) western coast of Australia, c) eastern coast of North America.	35-36
2.4.1	Conceptual design of the ocean based structure (overhead view).	41
2.4.2	Location of inlet gate relative to tide level for the land based system at very near sea level.	45
2.4.3	Conceptual design of the land based system above sea level	49
2.5.1	Summary of the microalgal atmospheric carbon dioxide capture and storage design options selected in Chapter 2.	51
3.3.1	Density as a function of temperature for salinities ranging from 30 to 50 PSU calculated using the equation of state.	58
3.3.2	Ocean water temperature and salinity depth profile at 29.2°S, 113.1°E.	60
3.3.3	Ocean water density depth profile (adjusted to one atmosphere pressure) at 29.2°S, 113.1°E calculated using the international one-atmosphere equation of state of seawater.	61
3.3.4	Density (adjusted to one atmosphere pressure) as a function of depth for the water inside the pipe and the ocean column outside the pipe.	62

List of Figures (cont'd)

Figure No.	Description	Page No.
3.3.5	Two reservoir system where fluid 1 is in reservoir 1 and fluid 2 is in reservoir 2. The fluids meet at the interface.	63
3.4.1	Conceptual ocean disposal pipe system.	69

Chapter 1

Introduction

1.1 Greenhouse Gas Emissions and Climate Change

Increasing anthropogenic greenhouse gas emissions since the start of the industrial era have significantly increased the concentration of greenhouse gases in the atmosphere. Modeling studies have indicated the potential of a dramatic effect on the Earth's climate due to an increase in radiative forcing. Numerous early signs of climate change, such as reduced ice pack and warmer temperatures in the Arctic, are cited as examples of effect (Meehl et al. 2007). An increase in the greenhouse gas concentrations in the atmosphere has caused an increase in the atmospheric absorption of outgoing radiation, commonly called the greenhouse effect. Carbon dioxide has the highest net contribution of all the greenhouse gases to radiative forcing despite its low global warming potential relative to other greenhouse gases because of its higher concentration in the atmosphere. Atmospheric carbon dioxide levels have increased from 280 ppm in 1750 to 379 ppm in 2005 compared to an increase of only 20 ppm over the previous 8000 years before 1750 (Solomon et al. 2007). The increase in radiative forcing has caused an increase in global temperatures, commonly called global warming. The global surface temperature has increased by 0.76 ± 0.19 °C from 1850-1899 to 2001-2005 (Solomon et al. 2007). Examples of the impact of temperature change include changes in ocean temperature, snow and ice cover, and precipitation patterns.

The heat content of the upper 700 meters of the global ocean has increased by $10.9 \pm 3.1 \times 10^{22}$ J over the period of 1955 to 2003 (Bindoff et al. 2007). Increase in heat content causes thermal expansion of sea water; therefore, an increase in ocean heat content has increased the volume of the oceans and helped contribute to sea level rise. Over the period of 1993 to 2003, the rate of global mean sea level rise was estimated as 3.1 ± 0.7 mm yr^{-1}, of which approximately 52% is estimated to be from

thermal expansion of the oceans (Solomon et al. 2007). Also contributing to ocean rise is the change in land ice such as the loss of glacier, ice cap and ice sheet mass due to increasing temperatures. The change in land ice from 1991 to 2003 is estimated to be 1.2 ± 0.4 mm yr^{-1} in sea level equivalent (SLE). The balance of the change is from unknown sources (Solomon et al. 2007).

Warming of the Earth's surface has led to increased evaporation and an increase in the amount of moisture air can contain. The change in evaporation rate and specific humidity has led to changes in the intensity, frequency and type of precipitation occurring throughout the world. Observed trends from 1900 to 2005 indicate that some regions of the world are experiencing more precipitation while others have become drier. However, even in areas with less precipitation more heavy or extreme precipitation events are occurring (Trenberth et al. 2007).

There exist various options for reducing anthropogenic carbon emissions and for reducing the concentration of carbon in the atmosphere. The majority of these options fall into one of four categories: i) reduced energy consumption, ii) less carbon-intense and near zero-carbon energy sources, iii) carbon dioxide capture and storage, and iv) enhancement of natural sinks. The first three options reduce carbon emissions, while the latter one reduces the concentration of atmospheric carbon.

Reducing energy consumption reduces carbon emissions when the energy source is a fossil fuel. Reducing energy consumption can be achieved by improving energy efficiency of a supply-side or demand-side process. Reducing energy consumption can also be achieved by switching to less energy-intensive activities.

Using low-carbon and near zero-carbon intensive energy sources in place of high-carbon energy sources reduces carbon emissions since less carbon is produced per unit of energy produced. For example, compared to using coal to generated

electricity, natural gas is a low-carbon energy source and biomass is a near zero net carbon energy source.

Enhancing natural carbon sinks decreases atmospheric carbon by removing carbon from the atmosphere and storing it in other reservoirs. Two natural carbon sinks of interest for enhancement are the biosphere and the hydrosphere. The biosphere is defined here as the total of all living organisms on Earth. An increase in the amount of terrestrial biomass will reduce the carbon content of the atmosphere. The hydrosphere is all water on Earth, including the ocean, lakes, rivers, ice, and clouds. Similarly, increasing carbon uptake of the hydrosphere can be achieved by a long term increase in the carbon content of the oceans.

Carbon dioxide capture and storage reduces atmospheric carbon levels by storing the carbon in a location other than the atmosphere. Capture and storage generally involves capturing the carbon dioxide emissions from an industrial process before it is released to the atmosphere and injecting the carbon dioxide in an underground geological formation or in the ocean. However, it can also be realized by a method of removing carbon from the atmosphere itself and storing it.

The reduction of carbon emissions and carbon levels in the atmosphere to a stable level will likely be the result of a combination of the four options rather than of one single option.

1.2 Objective of this Thesis

The objective of this thesis is to evaluate a specific system which captures carbon dioxide from the atmosphere and transfers it to a location of long term storage. Growing algal biomass was selected as the method for capturing atmospheric carbon dioxide and the deep ocean was selected as the storage location. A method for disposing carbon in the deep ocean was developed and a number of different options for growing biomass were investigated.

A conceptual physical scope of microalgal growth and disposal systems is developed to define all of the steps required to sequester atmospheric carbon in the deep ocean. Since multiple processes are operating at the same time, e.g. evaporation, photosynthesis and diffusion of carbon dioxide, the rates of each process are considered in order to define the rate limiting step. Finally the capital cost is analyzed to test the economic feasibility of the process compared to other means of carbon sequestration.

1.3 Background

1.3.1 Microalgal Atmospheric Carbon Dioxide Capture and Storage

Photosynthesis is the complex process by which organisms convert energy from sunlight, carbon dioxide and water into oxygen and organic carbohydrates; these are called phototrophic organisms. The majority of phototrophic organisms absorb light energy in green pigments called chlorophyll. Carbon dioxide is absorbed by terrestrial plants through their leaves and by phototrophic aquatic organisms through their cell membranes.

The products of photosynthesis are carbohydrates, oxygen and water. The oxygen produced is released into the atmosphere while the carbohydrates are either used directly in respiration or converted into lipids, protein or other carbohydrates. Glucose is one of the carbohydrates produced in photosynthesis, and is approximately 44% carbon by weight which helps contribute to the relatively high carbon content in biomass. In most cases, biomass is composed of 45% to 50% carbon based on dry weight measurements (Schlesinger 1991). The relatively high carbon composition of biomass makes it a suitable medium for short term storage of carbon.

The rate of carbon uptake by biomass is specific to a crop and an environment. For example, corn averages a carbon uptake of 6 g m^{-2} d^{-1} or a total average biomass production of 13 g m^{-2} d^{-1} dry weight, assuming a 100 day growing season as typical (Blanco-Canqui et al. 2006). Stern cites that 0.4 ha of corn accumulates 2500 kilograms of carbon per growing season, or approximately 6 g m^{-2} d^{-1} of carbon (Stern, Jansky, and Bidlack 2003).

Numerous types of photosynthetic organisms exist on the Earth, with many unique physical and chemical properties. However, it was determined that algae were the best suited for capturing atmospheric carbon dioxide and transferring it to a site of long term storage. Algae are "thallophytes (plants lacking roots, stems, and leaves) that have chlorophyll *a* as their primary photosynthetic pigment and lack a sterile covering of cells around the reproductive cells" (R. E. Lee 1989). Algae are generally found in marine and freshwater environments but can also be found in nearly all other environments on Earth. The size of algae ranges from 0.2 to 2.0 μm in diameter for microscopic picoplankton to lengths of up to 60 m for giant kelp (Barsanti and Gualtieri, 2006). Only microalgae will be considered in this thesis for use as the means of capturing atmospheric carbon dioxide. Microalgae can be defined as the "microscopic algae *sensu stricto*, and the oxygenic photosynthetic bacteria, i.e. the cyanobacteria" (Tomaselli 2004).

Microalgae were regarded as the best form of biomass for atmospheric carbon dioxide capture and storage because they have various characteristics that are superior to other forms of biomass in all aspects of carbon dioxide capture and storage. Microalgae are effective at capturing carbon because they grow at relatively high growth rates and have been commercially produced on large scales with relatively low labour. Microalgae can also be effectively stored in the long term, especially in the deep ocean, as discussed further below, since they are non-buoyant, grow in aquatic or marine environments, are small in size, and can be grown at high salinities.

Climate is one important factor that affects microalgal growth rate and therefore productivity of outdoor microalgal systems since it determines the amount of sunlight available and the temperature of the culture (Oswald 1988). Sunlight provides the energy needed by microalgae to perform photosynthesis and can inhibit growth if it is not available in sufficient amounts. Microalgal growth occurs at an optimal temperature which is species dependant. The optimal growth temperature is only known for a limited number of microalgal species and ranges from 20°C to 32°C (Oswald 1988).

The most important factors affecting productivity that are directly related to pond design are carbon dioxide addition and mixing. Carbon dioxide is necessary for photosynthesis and can be added to cultures as a pure stream or solely from diffusion from the atmosphere. Turbulent mixing is important in microalgae cultures because it prevents settling and photoinhibition. In some systems mixing can also enhance carbon dioxide transfer into the culture medium. Settling occurs when the flow of the culture medium is too slow and the algae sink to the bottom of the pond. Settling can cause algae cells to die, reducing productivity. Photoinhibition is the decline of photosynthetic rates due to prolonged exposure to above optimal irradiance (Masojidek, Koblizek, and Torzillo 2004). Mixing prevents photoinhibition, and thus the decrease in productivity it causes, by rapidly moving the microalgal cells back and forth from the photic zone to the lower unilluminated or less illuminated layer (Richmond 1986). In systems dominated by wind driven mixing, this type of mixing can increase carbon dioxide transfer into the culture medium by increasing gas exchange between the atmosphere and the pond water. Gas exchange increases significantly over a range of typical wind speeds, e.g. by approximately 3 times when wind speeds increase from 0 to 5 m s^{-1} (see Chapter 4 for more details).

As discussed further below in Section 2.2, the productivity of large scale microalgal production systems range from approximately 1 to 25 g m^{-2} d^{-1} of dry weight biomass. The productivity of corn is 13 g m^{-2} d^{-1} dry weight, which falls near the middle of the range of productivities of microalgae.

The large scale cultivation of microalgae requires less labour than the cultivation of conventional land based crops. Land based agriculture requires a considerable usage of large man operated machinery to seed, fertilize, and harvest crops. Pumps and piping are used to carry out these similar processes for large scale production of algae which significantly reduces labour.

While microalgae are effective at capturing dissolved carbon dioxide they are not effective at storing it in the long term unless the biomass is sequestered. Bacteria and other decomposers obtain energy by decomposing organic matter such as biomass and in the process release the carbon contained in the biomass back into the atmosphere in the form of carbon dioxide. Therefore the carbon captured by biomass will be re-released to the atmosphere if the decaying biomass is left exposed to biological processes that are in turn exposed to the atmosphere for too long of a time period. In nature the carbon in biomass is not sequestered; complex ecological webs recycle the carbon to the atmosphere as living organisms use the energy. For solid biomass, there is no obvious method for long term storage of the organic carbon. For example, it would be difficult to pump material such as wood or straw into a geological formation as is being proposed with captured carbon dioxide from industrial processes. However, the deep ocean has the potential to store carbon and keep it isolated from the atmosphere for a number of centuries, as discussed further below, provided the biomass remains in the deep ocean, i.e. does not float back to the surface.

Microalgae can be more effectively transported and stored in the deep ocean than other forms of biomass. Since microalgae are small in size and grow in water they

can be more easily transported through piping than other forms of biomass. Land based biomass would need to be added to a carrier fluid in order to be transported by pipeline and further suffers from the problem that almost all solid biomass is less dense than sea water unless submerged for lengthy periods of time. Hence solid biomass that was transported into the deep ocean would migrate to the shallow ocean, and decay or predation of the material would return carbon to the atmosphere. Marine microalgae, by contrast, are already grown in a suitable carrier fluid, sea water, and are not buoyant in sea water when not exposed to light. Hence marine microalgae transported into the deep ocean would not rise through the ocean water column.

1.3.2 Ocean Water Density and Temperature Variation

Approximately 7.2 ± 0.3 GtC yr^{-1} are released to the atmosphere from the burning of fossil fuels each year of which 4.1 ± 0.1 GtC yr^{-1} remains in the atmosphere. The remaining 3.1 ± 1.1 GtC yr^{-1} is taken up by the ocean (2.2 ± 0.5 GtC yr^{-1}) and by the biosphere (0.9 ± 0.6 GtC yr^{-1}) (Solomon et al. 2007). The intermediate and deep layers of the ocean contain approximately 38,000 Gt of carbon (Doney, Lindsay, and Moore 2003). If the anthropogenic carbon that remained in the atmosphere from yearly emissions were removed to the deep ocean, the concentration of carbon in the deep ocean would only increase by 0.01%. Because of the very small amount of anthropogenic carbon in the atmosphere compared to the amount in the deep ocean, and because the deep ocean is not saturated in carbon, there does not appear to be a practical limit on the amount of carbon that can be stored in the deep ocean.

Because of the layering of the ocean, the deep ocean is separated from the upper layer and hence the atmosphere. A critical question is the length of time for which carbon in the deep ocean remains isolated from the atmosphere.

The density of the ocean increases with depth due to decreasing temperature and increasing salinity. However, the change in density does not occur at a constant rate over all depths of the ocean. The difference in density gradient causes the ocean to form three separate zones: the surface zone or mixed layer, the pycnocline zone, and the deep zone or deep ocean (see Figure 1.3.1). The mixed layer is adjacent to the atmosphere and is characterized by a very gradual change in density as depth increases. In most areas of the ocean the mixed layer extends to a depth of about 100 meters (Segar 1998). Note that the mixed layer is both in contact with the atmosphere and has a high rate of gas exchange due to surface winds, and hence tends to equilibrate with the atmosphere in terms of dissolved gas. Below the mixed layer is the pycnocline zone which is a zone of rapidly increasing density due to a rapid decrease in temperature and in some areas an increase in salinity. The pycnocline zone generally extends to depths of 500 to 1000 meters (Segar 1998). Below the pycnocline is the deep ocean which extends to the ocean floor. The change in density with depth in the deep ocean also occurs very gradually. Due to the lower temperature and very high pressure of the deep ocean, it is below saturation in dissolved gas content.

Since the pycnocline zone has a strong vertical density gradient large amounts of energy are needed to transfer mass through this zone. This severely limits vertical mixing of water masses, dissolved gases and chemicals in the pycnocline zone. Because the pycnocline zone acts as a barrier between the layers above and below it, it isolates the deep ocean from the upper ocean and the atmosphere.

While the density gradient of the pycnocline zone isolates the deep ocean from the atmosphere, the time scale at which matter stays in the deep ocean before returning to the upper ocean is determined by ocean circulation. Mass exchange from the surface to the deep ocean occurs at a limited number of locations in the oceans. These locations are at high latitudes where the pycnocline is much weaker since heat loss from the ocean is higher than heat gain from solar irradiance (Marshall and

Schott 1999). At these regions surface water density is increased due to low temperatures and increased salinity. There are two reasons for increased salinity. The first is ice exclusion in which ice with a lower salt content is formed and a higher salinity brine is rejected to the surface ocean. The second reason is high evaporation in water flowing to some regions of high latitude, as occurs in the Atlantic Ocean (Segar 1998). The Mediterranean Sea has a high rate of evaporation relative to rainfall, and as a result a high salinity current flows out of the Mediterranean and across the Atlantic, to join the Gulf Stream current flowing to the northern Atlantic Ocean. As this water cools, its high salinity contributes to the overall high density that causes downwelling currents in the Greenland Iceland Norway (GIN) area. The combination of the weak pycnocline and high density allows the surface water to sink to the deep ocean. Major areas of deep convection occur in the Labrador, Greenland and Weddell Seas (Marshall and Schott 1999).

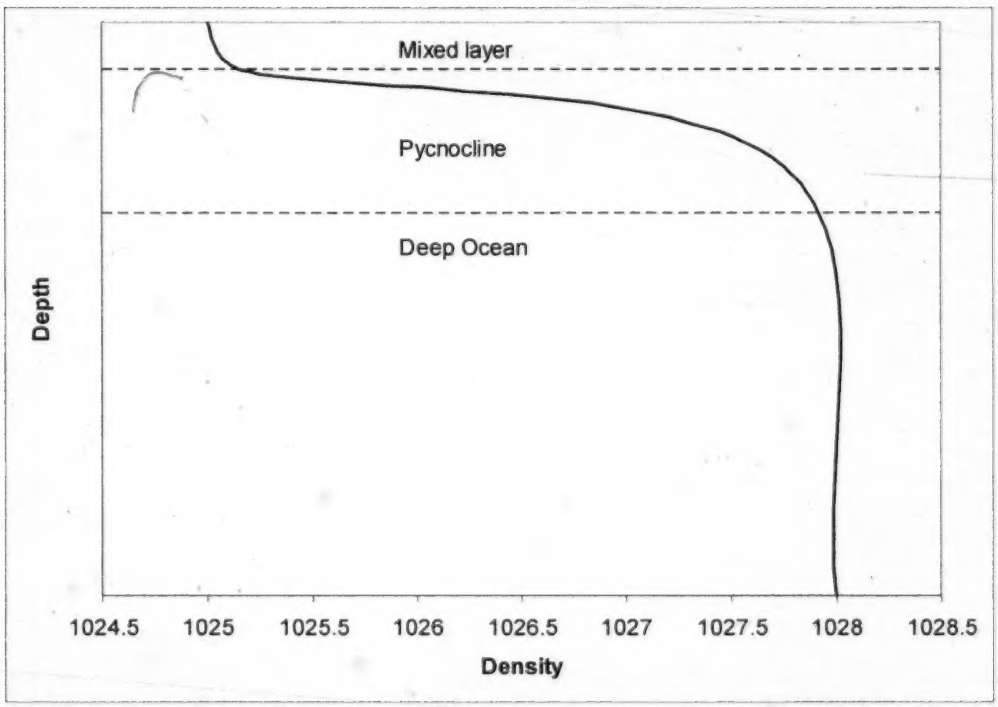

Figure 1.3.1: Generalized density depth profile of the ocean showing the mixed layer, the pycnocline zone, and the deep ocean.

Once the surface water reaches the deep ocean through deep convection it is transported horizontally and eventually returned to the surface by mixing and upwelling. The overall circulation is known as thermohaline circulation (or the ocean conveyor belt), and the amount of water moved by thermohaline circulation determines the average residence time of water in the deep ocean. This time period has been estimated between 300 and 1000 years (Caldeira et al. 2005) which makes the deep ocean a suitable location for long term storage of captured atmospheric carbon.

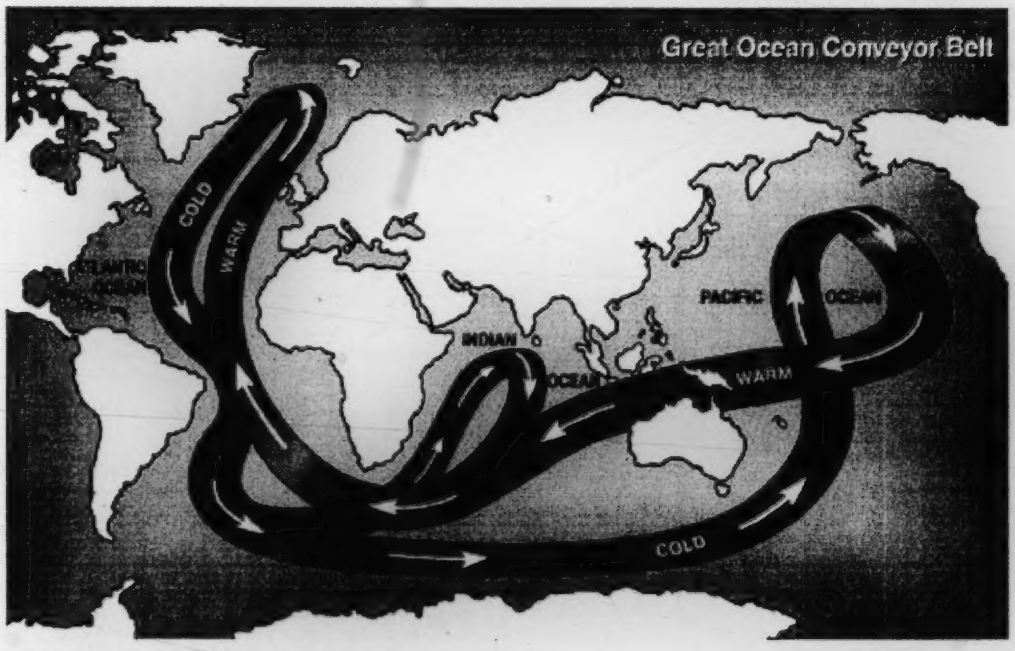

Figure 1.3.2: The Ocean Conveyor Belt (http://science.nasa.gov/headlines/y2004/05mar_arctic.htm).

1.3.3 Ocean Topograhpy

The process of disposing carbon into the deep ocean is affected by the relationship of land and ocean. The distance to the deep ocean from the coast depends on the size of the continental margin. The continental margin consists of the continental

shelf, continental slope and continental rise. Continental shelves are relatively flat plains that are adjacent to the coastline. Continental shelves typically slope seaward at approximately 0.5 degrees and have an average width of 60 km. However, the width of continental shelves has a wide range, from a few kilometers to over 1000 km. On the west coast of the Americas, and in particular off the coast of South America, shelves are relatively narrow, while in the Arctic and in the Grand Banks area of the Atlantic Ocean the shelf is very wide.

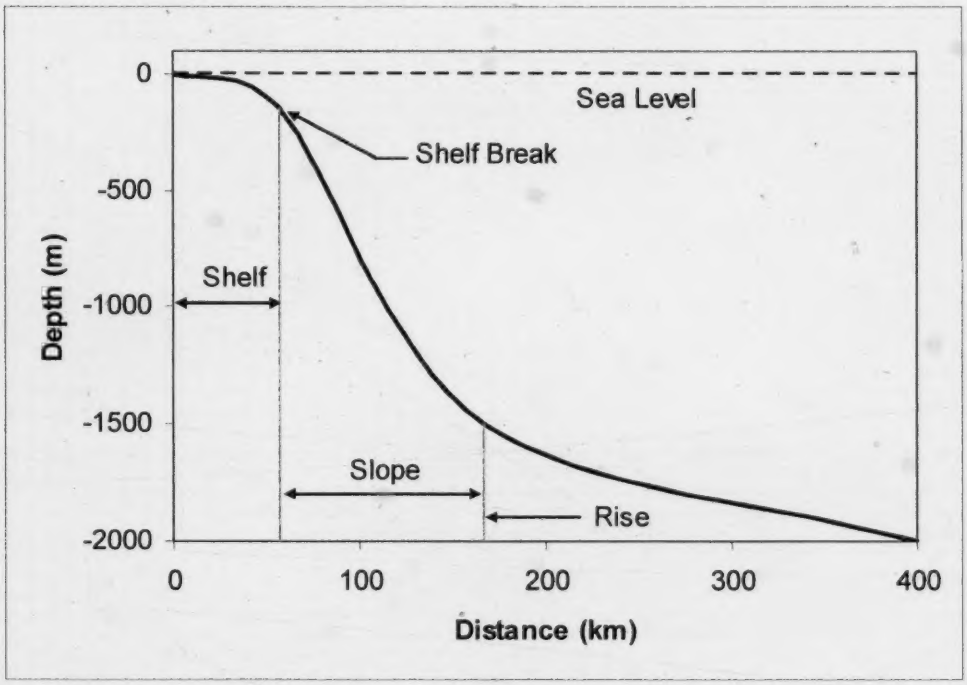

Figure 1.3.3: Generalized profile of the continental margin showing the continental shelf, slope, and rise.

Continental shelves end at the shelf break, which occurs at an average ocean depth of 130 m but can be as deep as 200 m. At the shelf break the drop in the level of the ocean floor increases; this area is known as the continental slope. The continental slope has an average slope of approximately 4 degrees and extends to depths of 2 to

3 kilometers where it meets the continental rise. The width of the continental slope is generally less than 150 km.

The continental rise is a large underwater plain with slopes of generally less than 1 degree. Continental rises can extend for as far as 500 km and can reach depths as great as 4 kilometers where they connect with the abyssal ocean, i.e. areas of great depth up to eight km.

Access to the deep ocean requires that one be sufficiently past the shelf break to a point where the ocean floor is below the pycnocline.

1.4 Organization of the Thesis

In this work we will review the potential of microalgal growth and transport to the deep ocean as a means of long term sequestration of atmospheric carbon. In Chapter 2 systems for growing microalgae are reviewed in detail, followed by an analysis of how these might be applied at a very large scale for the growth of microalgae for disposal into the deep ocean. In Chapter 3 methods of economically disposing microalgae to the deep ocean are developed. In Chapter 4 potential rate limiting factors of the capture and storage of carbon dioxide using microalgae are evaluated. In Chapter 5 the feasibility of these atmospheric carbon dioxide capture and storage systems relative to other means of carbon sequestration is evaluated. In Chapter 6 we develop conclusions from this work and suggestions for further research.

Chapter 2

Microalgal Atmospheric Carbon Dioxide Capture and Storage System Options

2.1 Microalgal Species for Commercial Production

2.1.1 Overview

Microalgae are mostly produced commercially for human nutrition. Various species of microalgae that are produced commercially are included in various food products including pastas, snack foods, candy bars, gum, beverages and supplements. The microalgae are added to the food products either for nutritional benefit or as a natural colourant. Microalgae are especially used as a source of protein in human nutrition since some species are composed of up to 71% protein (dry weight) (Becker 2004). It was the search for alternative sources of protein that helped lead to the development of commercial production of microalgae. Microalgae are also marketed as health foods in various forms including tablets, capsules, and liquids. The alleged health benefits from microalgae consumptions are numerous and species dependant; these health benefits will be briefly discussed for two microalgae species in Sections 2.1.2 and 2.1.3. Microalgae are also used as natural colouring agents in human nutrition (see Section 2.1.4 for an example).

Another common use for microalgae is as feed for aquaculture and animals. Microalgae are used as feed in aquaculture for their nutritional value and as a colouring agent in some species such as salmonids (the family of fish to which salmon belong). Microalgae are easily incorporated as feed in aquaculture since they are a natural food source for many of the species grown. The majority of microalgae used as aquaculture are fed to mollusks (62%) followed by shrimp (21%) and fish (16%) (Spolaore et al. 2006). The usage of microalgae as animal feed is estimated to be 30% of world commercial microalgal production (Becker

2004). The types of animals which have microalgae incorporated into their food include pets such as cats, dogs, aquarium fish, and ornamental birds, and livestock such as cows, breeding bulls, horses, and poultry.

Commercial microalgal production plants exist in numerous countries in the world including Australia, China, Germany, Israel, Japan, and the United States. The three most common species of microalgae produced in large scale cultures are *Chlorella*, *Spirulina*, and *Dunaliella*. These three species are the most commonly produced since they can be converted into a product with a high price per unit weight. Another factor which makes them viable for commercial production is their ability to effectively grow in mass culture as a (nearly) monoalgal culture with limited competition and contamination when they are grown in highly selective environments, since they are able to out compete other organisms. Sections 2.1.2, 2.1.3, and 2.1.4 describe *Chlorella*, *Spirulina*, and *Dunaliella* in more detail, respectively.

2.1.2 *Chlorella*

The microalgae species *Chlorella* belongs to the group of green algae. Green algae are eukaryotes; eukaryotic cells are more complex organisms and have membrane-bounded organelles, whereas prokaryotic cells are simpler and lack membrane-bounded organelles (R.E. Lee 1989). Green algae species range from microscopic unicellular organisms to macroscopic multicellular organisms (Barasanti and Gualtieri 2006). Green algae differ from other prokaryotic species of algae since they form storage products, such as starch, in chloroplasts as opposed to the cytoplasm. *Chlorella* is a microscopic unicellular speices of green alga and is found in nearly all water environments (R.E. Lee 1989).

Chlorella is grown as a food source for humans, as animal feed and as feed for aquaculture. *Chlorella* contains little cellulose in its cell wall; because humans and non-ruminant animals cannot digest cellulose, more of the *Chlorella* cell can be

digested compared to other microalgal species which produce higher amounts of cellulose. *Chlorella* is a good source of protein since its cell contains approximately 50% protein (R. E. Lee 1989). *Chlorella* can be used as a food additive and is often promoted as a health food. *Chlorella* contains β-1,3-glucan which is claimed to be an active immunostimulator and to provide other health benefits (Iwamoto 2004). *Chlorella* used as feed for aquaculture especially used for growing rotifers (small planktonic animals) and fingerlings (young fish) which are in turn used as feed for larger fish.

Chlorella is successfully grown at commercial scales since it grows faster than other microorganisms in culture and easily outgrows them. The rapid growth rate of *Chlorella* allows it to dominate other species when grown in a medium that is nutrient rich, resulting in very little contamination.

Production of *Chlorella* is carried out mostly in Japan, Taiwan, Malaysia, Indonesia, and Germany. The annual production of *Chlorella* in the 1990s was approximately 2000 t (Iwamoto 2004) with annual sales of approximately US$ 38 billion. The world's largest *Chlorella* producer, located in Taiwan, produces 130 to 150 t of dry biomass per year (Spolaore et al. 2006). The systems used to produce *Chlorella* commercially will be discussed in Section 2.2.

2.1.3 *Spirulina*

Spirulina (or *Arthrospira*) is a blue-green alga (or cyanobacterium). Blue-green algae are prokaryotic, that is they lack membrane-bounded organelles. Since blue-green algae are prokaryotic they are more closely related to prokaryotic bacteria than to eukaryotic algae and it is debatable whether they should be included in the study of algae (phycology) (R.E. Lee 1989). Blue-green algae will be considered microalgae in this thesis since they perform the same function as microscopic eukaryotic algae in that they carryout photosynthesis using sunlight and inorganic carbon.

Blue-green algae species are either unicellular or multicellular and are found in both freshwater and marine environments. *Spirulina* is a multicellular blue-green algae which is found in a number of different environments especially alkaline, brackish, and saline waters.

Spirulina is mostly produced for human nutrition and as animal feed. *Spirulina* has a long history of human consumption. Dating back as far as possibly the 9th century in Chad and the 14th century in Mexico, indigenous peoples in these areas would harvest naturally growing *Spirulina* from alkaline lakes for the use in their diets (Barsanti and Gualtieri 2006). *Spirulina* has good nutritional value because of its high protein content, which can be as high as 65% (dry weight) and because it contains essential fatty acids, vitamins, and minerals (Hu 2004). *Spirulina* based products for human nutrition are sold as tablets, powders, chips, pasta, and liquids and is often marketed as a health product since it is claimed that *Spirulina* can reduce cholesterol, enhance the immune system, and help prevent tumor development, among others. Over 50% of world *Spirulina* production is used as animal feed for pets including cats, dogs, aquarium fish, and ornamental birds, and livestock including cows, breeding bulls, horses, and poultry (Spolaore et al. 2006).

A high pH and bicarbonate concentration is required for the growth of *Spirulina*. The high pH of the environments that *Spirulina* thrives in make it difficult for other microorganisms to survive thereby allowing *Spirulina* to out compete the other microorganisms and grow with very little contamination. The high pH environment that *Spirulina* grows in is key to maintaining a successful large-scale monoalgal culture.

The majority of *Spirulina* production plants are located in Asia but there are plants also located in California and Hawaii. The annual world production of *Spirulina* was estimated to be 2000 t in 2000 (Hu 2004) with the world's largest producer,

located in China, producing 200 t of dry biomass per year (Spolaore et al. 2006). The systems used to produce *Spirulina* commercially will be discussed in Section 2.2.

2.1.4 *Dunaliella*

Like *Chlorella*, *Dunaliella* is a unicellular green alga. *Dunaliella* is primarily found in bodies of water with more than a 2 molar concentration of salt, including ocean waters, brine lakes, salt marshes, salt lagoons and salt water ditches. *Dunaliella* is the most halotolerant (able to grow in high concentrations of salt) eukaryotic photosynthetic organism known and can grow in salt concentrations from 0.1 M to greater than 4 M (Ben-Amotz 2004).

Dunaliella, in particular the strain *Dunaliella salina*, produces the highest amount of β-carotene of all know microalgae, with β-carotene quantities reaching as high as 14% dry weight of the *Dunaliella* cell (Borowitzka and Borowitzka 1988). *Dunaliella* is produced commercially since it is a good source of β-carotene and is marketed either as β-carotene extracts, *Dunaliella* powder for human use, or as dried *Dunaliella* for animal feed. β-carotene is used in human nutrition as a natural food colourant and is often marketed as a health food. The health benefits of β-carotene include its ability to act as provitamin A, i.e. it is able to be converted to vitamin A. β-carotene is a good source of vitamin A for animals (including humans) since it is not toxic at high doses whereas vitamin A itself is. Some alleged health benefits of β-carotene include it being an antioxidant and being able to trap free-radicals which has been claimed to help prevent cancer and act as an anti-inflammatory. β-carotene is used in animal feed as a source of provitamin A, to improve coloration in animals including cattle, poultry, fish and shrimp and to improve the fertility of cattle.

Dunaliella is very suitable for commercial production in large outdoor ponds since it is able to thrive in a wide range of temperatures (from -5°C to greater than 40°C) with high solar irradiance in highly saline conditions using atmospheric carbon dioxide as the only source of carbon (Ben-Amotz 2004). The high salinity makes it difficult for other organisms to survive which allows *Dunaliella* to grow with limited predation and contamination.

Commercial production of *Dunaliella* is mainly carried out in Australia, China, India, Israel, and the U.S.A with the world's largest producer being situated in Australia. β-carotene products derived from *Dunaliella* sell for between US$300 to US$3000 per kg (Ben-Amotz 2004). The systems used to produce *Dunaliella* commercially will be discussed in Section 2.2.

2.1.5 Selection of Microalgae Species

In determining which microalgal species is most suitable for atmospheric carbon dioxide capture and storage the factor which is the most important is the environment in which the microalgal species can successfully be grown. The microalgae must be able to grown in a highly saline environment with high amounts of solar irradiance. The high salinity is necessary for two reasons. Firstly, large scale cultivation of microalgae requires large amounts of water and the ocean is a relatively cheap source of huge quantities of water. Section 2.3 provides greater detail of the systems requirements for growing microalgae for carbon dioxide capture and storage. Secondly, the salinity, and thus the density, of the ocean water based growth medium can be further increased by evaporation driven by solar radiation. A highly saline medium is important to deep ocean disposal, which will be discussed in greater detail in Chapter 3.

Growth rate is another important factor when determining which microalgal species to select since it determines the amount of carbon captured per area and time;

however, growth rate is more dependant on the type of system the microalgae is grown in than the species used. Section 2.2 provides more details on the type of systems used for large scale cultivation of microalgae and the growth rates achieved by these systems.

Since *Dunaliella* can grow at higher salinities with high levels of solar irradiance compared to other microalgal species and because it has been successfully grown at large scales, it was selected as the microalgal species to be grown for carbon dioxide capture and storage for this thesis.

2.2 Systems for the Commercial Production of Microalgae

2.2.1 Overview

Microalgae produced in commercial production systems grow in water based media which contain other nutrients essential for growth. These nutrients are either added to the growth medium or are already contained in the medium depending on its source. Since sunlight provides the energy that drives microalgal growth, it must be available abundantly. In order to effectively use available solar energy and nutrients, a number of different systems have been designed, developed, and constructed in order to produce different types of microalgae.

Virtually all commercial production of microalgae is carried out in outdoor ponds with enclosed systems recently becoming more feasible. In general, there are four different modes of cultivating microalgae at large scales: extensive cultivation, intensive cultivation, semi-intensive cultivation, and highly intensive cultivation. Extensive cultivation uses no mechanical mixing and minimal control of the environment and generally occurs in large open unmixed ponds (see Section 2.2.2 for more details). Intensive cultivation requires that all factors affecting cell growth and chemistry be controlled. Intensive cultivation is usually carried out in mechanically mixed circular ponds (see Section 2.2.3 for more details), raceway

ponds (see Section 2.2.4 for more details) and stirred tank fermentors (see Section 2.2.5 for more details). Semi-intensive cultivation lies between extensive and intensive cultivation. No mechanical mixing is utilized in semi-intensive cultivation; however partial control of growth factors is employed. Semi-intensive cultivation is carried out in large open unmixed ponds similar to those used for extensive cultivation but are usually smaller in size (see Section 2.2.2 for more details). Highly intensive cultivation, similar to intensive cultivation, controls all factors affecting growth but to a higher degree. This highly controlled cultivation occurs in enclosed photobioreactors (see Section 2.2.6 for more details).

The majority of commercial microalgal production systems grow microalgae under autotrophic conditions; however some systems operate under heterotrophic and mixotrophic conditions. In autotrophic growth conditions the microalgae carries out photosynthesis to grow using energy obtained from sunlight and carbon dioxide as the source of carbon. In heterotrophic growth conditions the microalgae obtains the energy and materials needed for growth from organic compounds. Heterotrophic production of microalgae can be carried out in the dark since energy is not obtained from sunlight. Mixotrophic growth conditions are a combination of autotrophic and heterotrophic conditions where the microalgae using both organic compounds and carbon dioxide coupled with sunlight for growth. A number of microalgal species can be grown in heterotrophic conditions, and thus mixotrophic conditions, including *Chlorella*. While heterotrophic and mixotrophic growth are not important to this thesis since they do not use carbon dioxide, they will be further discussed in Section 2.2.5 to help evaluate the different potential systems for microalgal carbon dioxide capture and storage.

2.2.2 Unmixed Ponds

Unmixed ponds are large ponds where no mechanical mixing occurs. While no mechanical mixing is performed on unmixed ponds, mixing does occur in these ponds by wind driven mixing. Unmixed ponds can be either natural lakes where

large natural blooms of microalgae grow or large lagoon-type ponds used specifically to grow microalgae.

Large natural blooms of harvestable microalgae can form on natural lakes when climatic conditions are suitable and sufficient nutrients are available. These microalgal blooms can thrive in particular when the characteristics of the lake water are selectively, for example due to high pH. Examples of natural lakes where large microalgal blooms form include a number of smaller lakes along the northeast border of Lake Chad in Africa and volcanic craters filled with alkaline water in Central Myanmar. The small lakes along Lake Chad are highly alkaline with a high pH which is suitable for the growth of *Spirulina* as nearly a monoculture. Some of the *Spirulina* that grows in these lakes is harvested near the shores by the Kanembu people as a source of food. Similar to the waters of the lakes that border Lake Chad, the waters of the old volcanic craters in Central Myanmar are highly alkaline and suitable for the growth of *Spirulina*. *Spirulina* from these lakes is collected by boat when the microalgal culture suspension is thick during the blooming season. At other times, the *Spirulina* is pumped and concentrated. After cultivation, the *Spirulina* from the alkaline craters is processed and sold as tablets. While the microalgae produced from the natural lakes in Africa and Myanmar are not true cultivation production systems, that is the microalgae harvested grows naturally, they produce a significant amount microalgal based product. For example, production of *Spirulina* from the alkaline craters in Myanmar is approximately 30 t per year (Y. K. Lee 1997).

Lagoon-type ponds used specifically for the production of microalgae are large unmixed ponds with either extensive or semi-intensive cultivation methods. While no mixing is done by mechanical means in these ponds wind driven mixing does occur. Carbon is not added to the growth medium in lagoon-type unmixed ponds but is obtained from the growth medium which is often supplied by ocean water, and by diffusion from the atmosphere. Unmixed lagoon-type ponds are of a simple

construction, using earth bermed walls to contain the growth medium. In semi-intensive unmixed ponds the salinity and nutrient supply (nitrogen, phosphorous and trace elements, but not carbon) is controlled to a greater degree than in extensive unmixed ponds and semi-intensive ponds tend to be smaller than extensive ponds. Also, the size of semi-intensive ponds are smaller, up to 5 ha with depths of approximately 20 cm (M.A. Borowitzka 1990) , compared to extensive ponds which can be as large as 250 ha with depths up to 50 cm (Tredici 2004). Unmixed lagoon-type ponds are almost used exclusively for the production of *Dunaliella* and have very low productivities, approximately 1 g m^{-2} d^{-1} dry weight (Tredici 2004), compared to other systems since no mechanical mixing is done and no carbon is added to the growth medium. Despite the low productivities of these systems they can be cost effective because of their simple construction and low operating costs, particularly when climatic conditions enable year-round operation. Unmixed lagoon-type pond production systems are in operation in Western Australia which produce *Dunaliella*, with the largest using 460 ha of multiple ponds to produce 7 to 10 t of β-carotene per year (Y. K. Lee 1997).

2.2.3 Circular Ponds

Circular ponds were among the first systems used for the commercial production of microalgae, having been established in the 1960s in Japan and Taiwan. Circular ponds used for the commercial production of microalgae are large circular shaped ponds that are generally constructed with heavy reinforced concrete. Continuous mixing is provided in these ponds by a centrally located motor powered rotating arm. Circular ponds operate in the intensive cultivation mode.

Circular ponds are often shallow with culture depths as small as less than 5 cm. The size of circular ponds is limited, however, by the amount of water resistance acting on the motor which rotates the mixing arm. The largest circular pond used for the commercial production of microalgae was reported to have a diameter of 50 m (Y. K. Lee 1997).

Compared to other production systems, circular ponds are not favourable for commercial production of microalgae because of the high cost of the heavy reinforced concrete used for their construction and because of the high energy requirement for the continuously operated mixing arm. Another disadvantage of circular ponds is that while mixing is continuously provided it does not occur evenly in the culture with very little mixing occurring at the center of the pond. Despite the disadvantages of circular ponds, they are still commonly used in Japan, Taiwan, and Indonesia to produce *Chlorella* because of their long history of use and familiarity with the technology.

2.2.4 Raceway Ponds

Raceway ponds are oblong shaped ponds divided in the middle along the length of the pond in order to divide the pond into two continuous channels. Raceway ponds can be constructed as earth bermed ditches covered with plastic lining or concrete blocks can be used to construct the channel walls, which are then covered by a plastic liner. The size of raceway ponds range from 1000 to 5000 m^2 and they have depths of rarely lower than 15 cm (Tredici 2004). A single paddlewheel is used in a raceway pond to produce flow in the channels of the pond. The velocity of the flow produced by the paddlewheel, or mixing velocity, is usually between 10 and 30 cm s^{-1} (Dodd 1986). The flow velocity helps create mixing in the medium and helps keep the microalgae cells in suspension.

Raceway ponds operate in the intensive mode of cultivation, therefore factors such as pH and water level are monitored and nutrients necessary for microalgal growth are added to the medium. Generally, carbon is added to the medium as a pure stream of carbon dioxide to enhance productivity. Well managed raceway ponds can achieve growth rates of up to 20 to 25 g m^{-2} d^{-1} dry weight for short periods of time but long term productivity is closer to 12 to 13 g m^{-2} d^{-1} dry weight (Tredici 2004).

Despite the relatively low capital costs and high productivities of raceway ponds, they still encounter some drawbacks. Since raceway ponds cannot operate at water depths of less than 15 cm, which would cause a decrease in flow and turbulent mixing, large volumes of water are required. The large volumes of water result in low cell concentrations which increase the risk of contamination and increase harvesting costs.

Raceway ponds are mostly used to produce *Spirulina* but production systems producing *Dunaliella* are also in operation. Raceway ponds are used to commercially produce *Spirulina* in Hawaii and California. The plant in Hawaii uses ponds with a total area of 7.5 ha to produce 380 t of *Spirulina* per year. The plant in California, the largest in the world that produces *Spirulina*, uses ponds with a total area of 15 ha to produce 500 t per year (Y. K. Lee 1997). Numerous production plants are in operation in China as well that use raceway systems to produce *Spirulina*. *Dunaliella* is produced in a raceway pond plant in Israel.

2.2.5 Stirred Tank Fermentors

Conventional stirred tank fermentors are used to produce microalgae heterotrophically and have been proposed for usage in mixotrophic production of microalgae. Under heterotrophic conditions microalgae do not use sunlight or carbon dioxide to grow but rather use organic sources of carbon which need to be added to the growth medium in the fermentor.

There are a number of advantages of using stirred tank fermentors to produce microalgae heterotrophically. Stirred tank fermentors are well understood and have a long history of design and operation. Another advantage of stirred tank fermentors is that high cell concentrations are achievable, which can help reduce harvesting and capital costs of the microalgae production system. Despite the advantages of using stirred tank fermentors to produce microalgae under

heterotrophic conditions, there are a number of disadvantages as well. Not all microalgal species can grow under heterotrophic conditions and therefore the use of stirred tank fermentors is limited by the type of species they can produce. Another disadvantage of fermentors is that the growth rate of most microalgae species that can be grown heterotrophically is less than their autotrophic growth rate.

Unlike most microalgal species, the heterotrophic growth rate of *Chlorella* is similar to its autotrophic growth rate. Because of this, the production of *Chlorella* under heterotrophic conditions in stirred tank fermentors is common, particularly in Japan. In these systems, the source of organic carbon is commonly acetate or glucose. The annual heterotrophic production of *Chlorella* in Japan was approximately 550 t in 1996 (Y. K. Lee 1997).

Mixotrophic microalgal production systems combine autotrophic growth and heterotrophic growth and have the same advantages as heterotrophic systems. Besides the same advantages as heterotrophic growth, the main advantage of mixotrophic production is the increased growth rate which is approximately equal to the sum of the autotrophic and heterotrophic growth rates. Mixotrophic production it is not being carried out at commercial scales however a number of experimental systems have been developed. Once such system which produced *Chlorella* used an indoor stirred tank fermentor during the night for heterotrophic growth and an outdoor tubular photobioreactor (see Section 2.2.6) during the day for autotrophic growth (Y. K. Lee 2001).

2.2.6 Photobioreactors

Photobioreactors (PBR) are enclosed systems where the majority of the light must pass through the surface of the photobioreactor before it reaches the microalgal culture. Since PBR are enclosed they severely limit the exchange of materials with the atmosphere, such as gases and contaminants. PBR are generally operated outdoors in order for the microalgae culture to use the energy from sunlight to

perform photosynthesis. PBR operate under highly intensive conditions with a high degree of control of growth factors including pH, temperature, carbon dioxide concentration and oxygen concentration. A number of different PBR designs have been proposed however very few PBR have been successfully operated for large scale commercial production of microalgae. The different designs of PBR generally fall into one of three categories: tubular photobioreactors, flat photobioreactors, or vertical cylinders.

Tubular photobioreactors use a series of small transparent tubes, called the photostage, where the microalgae culture undergoes photosynthesis. The culture medium is usually circulated using a pump or air lift to a separate vessel where gas exchange and nutrient addition occurs. Tubular photobioreactors are usually either serpentine photobioreactors where the tubes are connected in series by U-bends or they are manifold photobioreactors where the tubes are connected in series by a manifold at each end.

Flat photobioreactors are constructed of either transparent plastic or glass sheets which are used to create a panel and enclose the growth medium. Flat photobioreactors are generally separated into two types based on construction: flat alveolar panels and glass plates. Flat panels are constructed from plastic sheets and are partitioned internally to create channels within the panel; they are called alveolar because of the numerous channels per panel. Glass plates are constructed from glass sheets without internal separation. The thickness of the panels for both types of flat photobioreactor ranges from approximately 1.3 cm to 17 cm with the optimal panel thickness depending on the type of species being grown (Tredici 2004). Flat photobioreactors usually incorporate a number of panels connected together. The inclination of the panels depends on the system and can range from horizontal to vertical with any incline in between. Mixing is usually achieved in flat photobioreactors by circulating the growth medium using a pump and/or by air-bubbling.

Vertical cylinder photobioreactors are simple systems consisting of vertical columns constructed of either glass or plastic. When the columns are constructed of flexible plastic to form a sleeve or bag, the plastic is fixed to a rigid frame. The size of vertical cylinder photobioreactors typically ranges from 5 cm to 15 cm in diameter and 1.5 m to 2.5 m in height (Tredici 2004). Vertical photobioreactors can be operated either outdoors in natural light or indoors under artificial light. Mixing is generally achieved in vertical cylinder photobioreactors by injecting or bubbling air into the culture at the bottom of the column.

There are a number of advantages of using a closed photobioreactor system over an open system for commercially producing microalgae. The risk of contamination and predation are greatly reduced in photobioreactors compared to open systems which allow photobioreactors to be operated under a wider range of climatic conditions and also allows for a wider range of microalgal species to be cultivated. Better control of growth parameters, such as temperature, pH, and carbon dioxide concentration, is achievable in photobioreactors. Higher cell concentrations along with higher light utilization efficiency in photobioreactors generally lead to higher productivities in photobioreactors than in open systems. For example, *Spirulina* production in a serpentine reactor was 50 to 60% higher than in a raceway pond when produced under identical conditions (Tredici 2004).

Despite the advantages of photobioreactors, they have also have a number of disadvantages compared to open systems. Photobioreactors are susceptible to a number of problems which can lead to the failure of the photobioreactor if they are not carefully considered. These potential problems include overheating, oxygen accumulation, biofouling, cell damage due to sheer stress and deterioration of materials. Photobioreactors can be successfully designed and operated to overcome these difficulties; however, their main limitation is the difficulty in scaling up compared to open systems such as raceway ponds. The difficulty in scaling up

photobioreactors results in very high capital and operational costs. These high costs can cause the cost of microalgal production using photobioreactors to be an order of magnitude higher than when using an open pond system.

Only three photobioreactors systems have been successfully used to produce microalgae at a commercial scale for a significant period of time. Other PBR that have failed have done so either because of technical difficulties or because of high costs (Tredici 2004). One example of a PBR system to successfully produce the microalgae *Chlorella* at a commercial scale is in operation in Koltze, Germany. This 700 m^3 tubular photobioreactor uses a centrifugal pump to circulate the growth medium through glass tubes 48 mm in diameter. This system was designed to produce 150 t per year of dry biomass during its eight month growing season (Tredici 2004).

2.2.7 Selection of Microalgal Production System

In determining which microalgal production system is the most suitable for atmospheric carbon dioxide capture and storage the most important factor is the source of carbon dioxide used for microalgal growth. In order to capture atmospheric carbon dioxide for sequestration using a microalgal production system, the ultimate source of carbon dioxide used by the production system must be atmospheric carbon dioxide; it does not help to add other sources of carbon that do not ultimately reduce atmospheric carbon dioxide levels. This criterion quickly eliminates most microalgal production systems, in particular those that operate under intensive or very intensive conditions. Circular ponds, raceway ponds, stirred tank fermentors and photobioreactors are all designed to achieve a high rate of algal growth by the addition of carbon dioxide to the growth medium. Therefore these systems are not suitable for microalgal capture and storage of atmospheric carbon dioxide since they require the addition of sources of carbon from other than the atmosphere. This leaves unmixed ponds as the most suitable option for microalgal carbon dioxide capture and storage.

As previously discussed in Section 2.2.2, unmixed ponds are either natural lakes or lagoon-type ponds. Natural lakes are not suitable for microalgal carbon dioxide capture and storage since they are limited in location and limited in the type and amount of microalgae they can produce. Therefore unmixed lagoon-type ponds are the most suitable for microalgal carbon dioxide capture and storage.

Lagoon-type ponds also have lower capital and operating costs than most other microalgal production systems and have successfully produced the microalgal species *Dunaliella*, which was selected as the microalgal species to be utilized for this thesis as discussed in Section 2.1.5. Therefore, because of the suitability and advantages of unmixed lagoon-type ponds (referred to as unmixed ponds from this point forward), they have been selected as the microalgal production system for atmospheric carbon dioxide capture and storage for this thesis.

2.3 Geographic Location for Microalgae Production

2.3.1 Geographic Factors

Geographic location is very important to the construction and operation of the microalgal atmospheric carbon dioxide capture and storage system, having implications for both the unmixed pond microalgal production system and the deep ocean disposal system (discussed in greater detail in Chapter 3). The factors related to location that are important to the system include climate, terrain, and proximity to the ocean.

Climate affects both the productivity of the unmixed pond system and the deep ocean disposal system. The main climatic factors which affect productivity are solar irradiance, temperature, net evaporation (evaporation minus precipitation) and wind speed. The main climatic factor which affects the deep ocean disposal is net evaporation.

Solar irradiation is the most important climatic factor concerning the productivity of microalgae since it affects the amount of energy available for the microalgae to perform photosynthesis and it also affects the temperature of the growth medium. Solar irradiance generally is most intense at the equator and decreases as latitude increases towards the poles. However, solar irradiance that reaches the Earth's surface can also be reduced by cloud cover. Despite the high levels of solar irradiance in the tropics, many of these locations suffer from high cloud cover which reduces the amount of light available. Therefore a location with high irradiance and low cloud cover should be selected to maximize the amount of available sunlight available for the microalgae. Solar irradiance is also important to microalgal productivity since most microalgae species have an optimal growth temperature and solar irradiance provides thermal energy to the growth medium. An ideal location will have an ambient temperature that maintains the pond temperature at a consistent level, with no excessive loss through heat transfer, for example at night.

Net evaporation is important to both the productivity of the microalgal production system and for deep ocean disposal. High precipitation rates can severely dilute the nutrients of the low depth ponds which can lead to a drop in productivity and an increase in contamination from competing microalgae or predatory species. Contamination caused by high rates of precipitation can be a particularly problematic for *Dunaliella* since a sufficient decrease in salinity can allow other organism to compete against it. Excessive evaporation can lead to an increase in salinity and loss of water from the production system. An increase in salinity can decrease productivity however, it should not be fatal to *Dunaliella* since it can survive at equilibrium saturation levels of salt (Ben-Amotz 2004). Water losses due to high evaporation can be overcome with the addition of make-up water. Net evaporation is important to deep ocean disposal since as evaporation occurs, the salinity and thus density of water increases. The importance of the increase in density of water caused by evaporation for deep ocean disposal will be discussed in

greater detail in Chapter 3. Figure 2.3.1 is a plot of the net rate of evaporation for the month of October in the Pacific Ocean constructed from the National Oceanography Centre NOC1.1 Flux Climatology data (NOC 2008). Figure 2.3.1 illustrates the wide variation in global net evaporation and shows the high net evaporation rate off the west coast of Australia, which will be discussed further in Section 2.3.2.

Wind speed is also important to productivity since it provides mixing. As wind speed increases so does the carbon dioxide flux into the growth medium from the atmosphere which provides more carbon dioxide for microalgal growth. However, excessive winds can damage pond structures and introduce foreign materials into the growth medium such as bacteria (which can cause contamination) or dust (which can reduce light transmission).

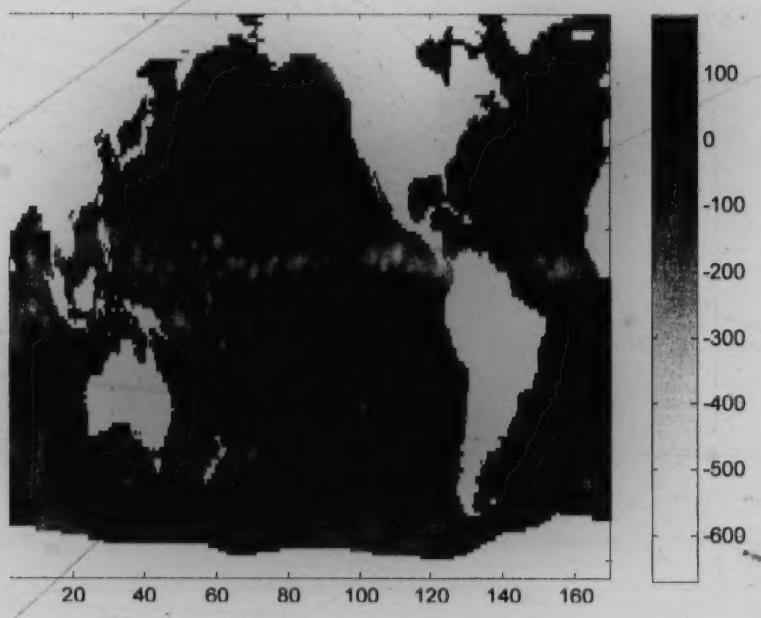

Figure 2.3.1: Net evaporation (mm per month) for the month of October in the Pacific Ocean; plot produced from data from NOC (2008).

Terrain is an important consideration for the construction of the unmixed pond microalgal system. Unmixed ponds require large areas of land in order to produce significant amounts of microalgae; the largest commercial unmixed pond production system is 460 ha. As will be shown in Chapter 5, a substantially larger area is required to have a significant impact on atmospheric carbon dioxide levels. Ideally, this large area of land should be relatively flat in order to minimize the amount of earth that needs to be moved in order to construct the earth bermed ponds.

Proximity to both the ocean surface and the deep ocean is important in considering the location of the microalgal atmospheric carbon dioxide capture and storage system. (The ponds will be located in low latitudes to benefit from high solar irradiance and net rates of evaporation. In this region of the ocean, the pycnocline is located about 500 to 1000 meters below the ocean surface. The depth to which the pycnocline extends at the location where the microalgae would be disposed into the deep ocean will be determined in Chapter 3). Since large amounts of water are required to grow microalgae, ocean water can be used as a vast and inexpensive source of water. Using ocean water as the growth medium is also desirable because of its salinity. Therefore the location of the microalgal carbon dioxide capture and storage system should be close to the ocean so that ocean water can be easily obtained for the system.

Close proximity to the deep ocean is also important in order to limit the distance in which the microalgae have to be transported from the production system to the deep ocean. In order to minimize the distance over which the microalgae is transported to the deep ocean, a location with a narrow continental margin should be selected for the microalgal carbon dioxide capture and storage system. Figure 2.3.2 is a topographical map of the ocean floor that shows the width of continental shelves constructed using the ETOPO2v2 database from the US National Oceanic and Atmospheric Administration (USDOC 2006).

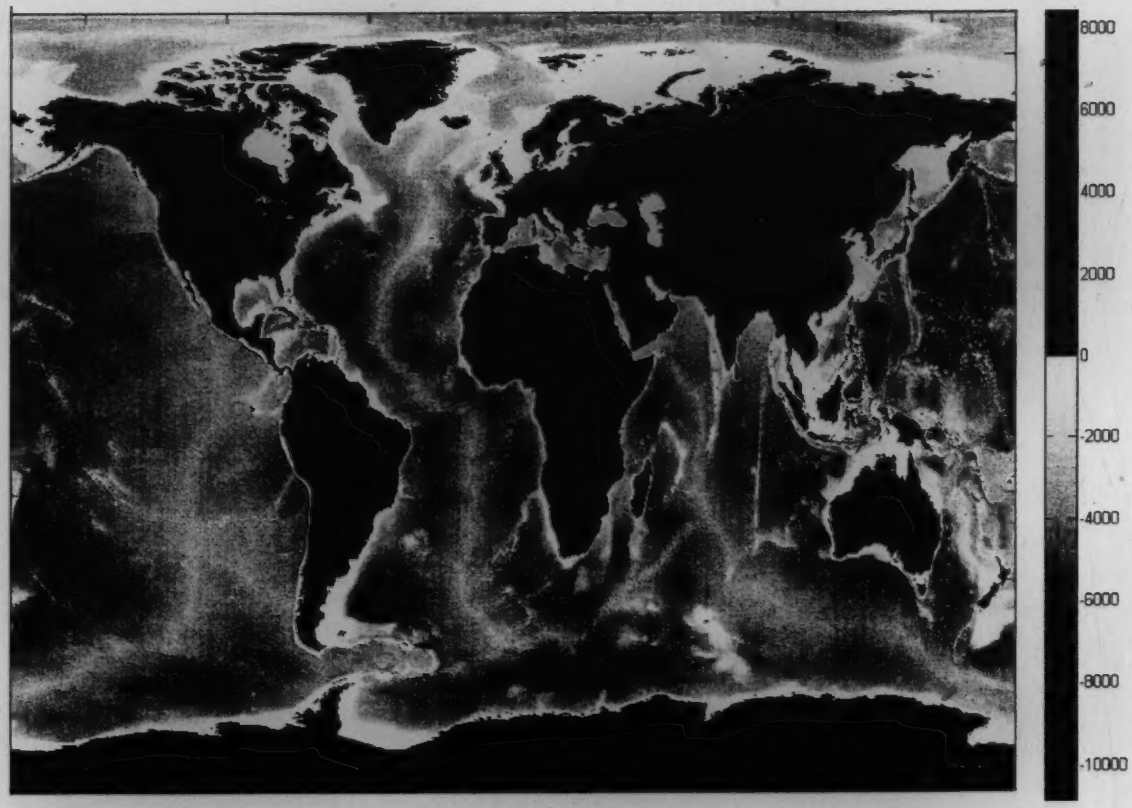

Figure 2.3.2: Topographical map of the ocean floor; plot produced from data from USDOC (2006).

The ETOPO2v2 database was also used to construct ocean floor profiles for locations off the western coasts of South America (Figure 2.3.3a) and Australia (Figure 2.3.3b) and the eastern coast of North America (Figure 2.3.3c). In these three figures the distance on the x-axis represents the distance seaward of shore with the distance of 0 km representing sea level. From these figures the wide range in the profile of the continental shelves can be seen. These profiles also show that, the location on the western coast of South America (Figure 2.3.3a) would provide access to the deep ocean at the shortest distance from shore followed by the location on the western coast of Australia (Figure 2.3.3b). Of these three locations, access to the deep ocean is furthest from the location on the eastern coast of North America (Figure 2.3.3c)

a) Western coast of South America

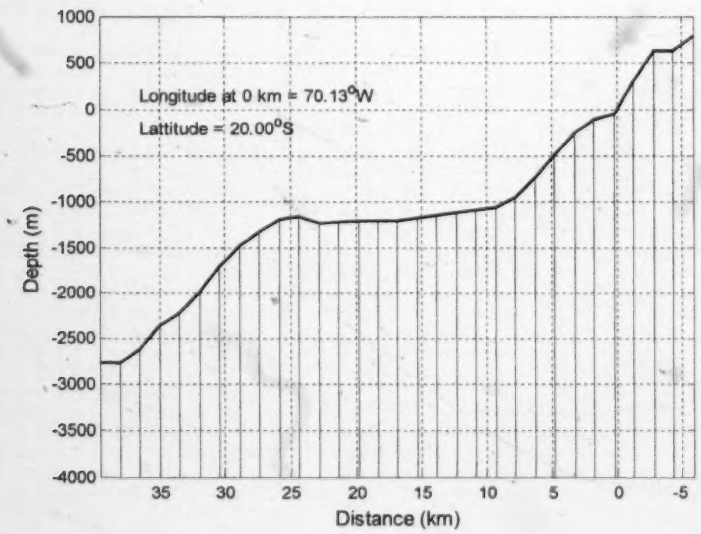

b) Western coast of Australia

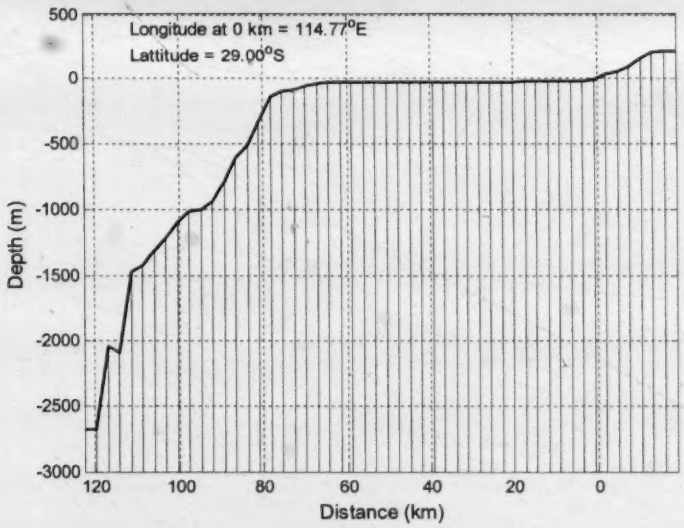

c) Eastern coast of North America

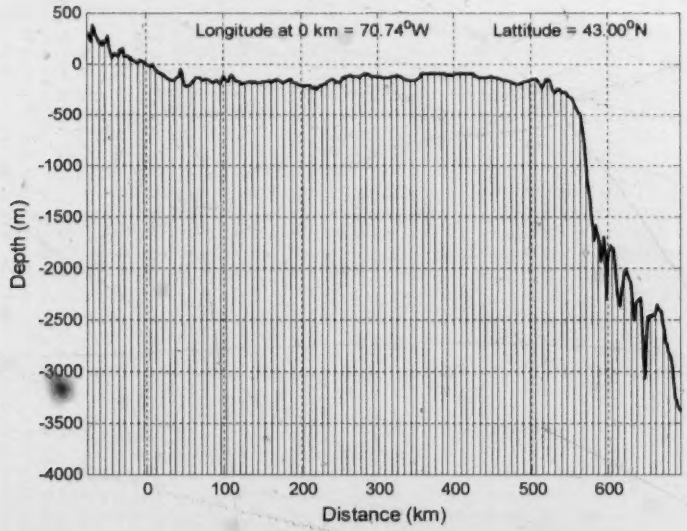

Figure 2.3.3: Ocean floor profile of three locations a) western coast of South America, b) western coast of Australia, c) eastern coast of North America; plot produced from data from USDOC (2006).

2.3.2 Selection of Geographic Location

The location selected in this study for the microalgal carbon dioxide capture and storage system was the west coast of Australia because of its favourable climatic conditions, its proximity to the ocean, and its narrow continental shelf. *Dunaliella* is produced commercially in Western Australia in large unmixed ponds using water pumped up from the ocean. Year round production is possible at this location because the climate is close to optimum with high light intensity, few cloudy days, minimal precipitation, and warm temperatures (L. J. Borowitzka 1991). Table 2.3.1 shows mean monthly and annual values for maximum temperature, minimum temperature, rainfall, evaporation, and wind speed for a location in Western Australia at 28.80° S and 114.70° E (COA 2007). The close proximity to the ocean allows for easy access to ocean water which is used as the growth medium. The distance to the deep ocean from the west coast of Australia is further compared to other coastal regions in the world such as the west coast of South America (see Figure 2.3.3). However an ideal location has to balance many factors, and Western Australia on balance is well suited as a base case.

Table 2.3.1: Mean monthly and annual weather statistics for 28.80° S, 114.70° E in Western Australia; source COA 2007.

Statistics	Jan	Feb	Mar	Apr	May	Jun	Jul	Aug	Sep	Oct	Nov	Dec	Annual
Mean maximum temperature (°C)	31.6	32.5	30.9	27.6	24	20.9	19.5	20	22	24.4	27.1	29.4	25.8
Mean minimum temperature (°C)	18.2	19.1	17.9	15.4	12.9	11	9.5	8.9	9.3	10.9	13.8	16.3	13.6
Mean daily rainfall (mm)	0.19	0.39	0.53	0.80	2.30	3.36	2.97	2.11	1.08	0.62	0.31	0.17	1.24
Mean daily evaporation (mm)	10.80	10.70	9.30	6.50	4.60	3.40	3.00	3.20	4.30	6.40	8.50	10.10	6.70
Mean daily net evaporation (mm)	10.61	10.31	8.77	5.70	2.30	0.04	0.03	1.09	3.22	5.78	8.19	9.93	5.46
Mean wind speed (m/s)	6.7	6.6	5.8	4.9	4.6	4.8	4.6	4.4	4.6	5.2	5.9	6.7	5.4

Terrain is another important consideration in determining the location of the microalgal carbon dioxide capture and storage system. The following Section (2.4) will discuss three different system designs.

2.4 Microalgal Carbon Dioxide Capture and Storage System Design Alternatives

2.4.1 Overview

This section describes three different conceptual alternate designs for the microalgal atmospheric carbon dioxide capture and storage system. The different designs are based on the different characteristics of the terrain on which they are built. The first design considered is not actually operated on land but rather on the ocean surface (see Section 2.4.2). The second design is a land based system operated at very near sea level (see Section 2.4.3). The third design is a land based system operated significantly above sea level (see Section 2.4.4).

2.4.2 Ocean Based System

A large flat area is required for the construction of the large unmixed ponds. The ocean surface offers a vast, relatively flat area on which a large structure incorporating unmixed ponds can be constructed for growing microalgae. Another advantage of an ocean based system is, that since it is on the ocean surface, the amount of pumping of ocean water into the ponds onto the ocean structure is minimized; in essence, the structure cells can be flooded rather than filled by pumping.

A number of large ocean based structure have been constructed in various parts of the world; these structures are generally referred to as very large floating structures (VLFS). Two different designs of very large floating structures exist: pontoon or semi-submersible.

Pontoon VLFS are flexible mat-like structures that float on the ocean surface with very little draft. Pontoon VLFS are highly stable in calm waters such as is found in sheltered coastal areas or small lakes. Breakwaters are usually placed around pontoon VLFS to reduce the height of waves that contact the VLFS. Pontoon VLFS generally have a mooring system in order to limit the amount they can drift. Pontoon type VLFS have been proposed as a more environmentally friendly alternative to land reclamation from the sea in order to increase usable space, especially in areas where land space is limited such as in coastal or island regions. Land reclamation from the sea can have a negative environmental impact on both coastal and marine ecosystems while it is claimed that VLFS do not damage ecosystems (Watanabe, Utsunomiya, and Wang 2004). A number of pontoon type VLFS that have been constructed including floating bridges in Japan, Canada, Norway, and the United States, a hotel in Vietnam and an amusement park in Japan. Note, however, that the requirement for shelter from ocean waves means that pontoon type VLFS are not well suited to applications in the open ocean.

Semi-submersible VLFS have a portion of their structure submerged beneath the ocean surface to a depth sufficient to dampen the response of the overall structure to surface waves, which limits the effect of waves and maintains a near constant buoyancy. Semi-submersible VLFS generally have a deck structure, floaters, and a submerged structure. For example, a series of submerged columns attached to the bottom of the hull can be used to limit the impact of waves on semi-submersible VLFS. One widespread application of semi-submersible VLFS is floating oil platforms. The largest VLFS built is the Mega-Float in the Tokyo Bay, Japan. The Mega-Float is a 2200 m by 300 m semi-submersible VLFS with a deck depth of 7 m supported by 320 submerged columns (Nakada and Suzuki 2004). The Mega-Float was constructed as a test model for a floating airport terminal and airstrip. Note that although this structure is a semi-submersible design, it is still sheltered behind breakwaters. Another interest in VLFS is their application as a Mobile Offshore

Base (MOB), a military support base deployed on the ocean surface. While a MOB has not yet been constructed a number of designs have been proposed for the US Department of Defense (Bender, Blair, and Ayyub 2001). Because semi-submersible VLFS withstand larger waves, they can be used in the open ocean.

The ocean based microalgal atmospheric carbon dioxide capture and storage system consisting of unmixed ponds constructed on a very large floating structure would use a single or series of vertical pipes to dispose of the microalgae into the deep ocean. The lengths of the pipes would have to be greater than the depth of the pycnocline therefore the VLFS would have to be situated in the open ocean away from the continental shelf. This would require that the VLFS be a semi-submersible VLFS in order to withstand the large waves that occur in the open ocean. Precise location of the VLFS would not be required, i.e. unlike an oil platform there would be no serious consequence if the VLFS drifted tens of kilometers off course. However, some positioning system would be required to keep the structure within a target area of the ocean, in order to maintain ideal climate conditions and the right depth for disposal of microalgae into the deep ocean.

The general design of the ocean based system incorporates a central circular section consisting of the down flow pipe or series of pipes. Connected to the central section and extending radialy from it are a series of channels which increase with width as the distance from the center increases (See Figure 2.4.1). The channels are the unmixed ponds where the microalgae grow. The channels are connected to the central pipe area by a vertically opening gate (the outflow gate) which is lifted to drain the microalgae into the pipe area for disposal in the deep ocean. At the opposite end from the outflow gate is the inflow gate, which also opens vertically. The inflow gate is used to fill the channels when it is lifted. In order for the channel to fill when the inflow gate is lifted the channel surface must be lower than the ocean surface once the gate is opened. In order to lower the inflow gate below the ocean surface for filling, a series of ballast tanks attached to the bottom of the

structure supporting the channels are required. The ballast tanks would fill with water in order to increase their density and lower the inflow gates below the sea surface level. The channels are not rigidly connected together so that the channels can be filled with ocean water at separate times.

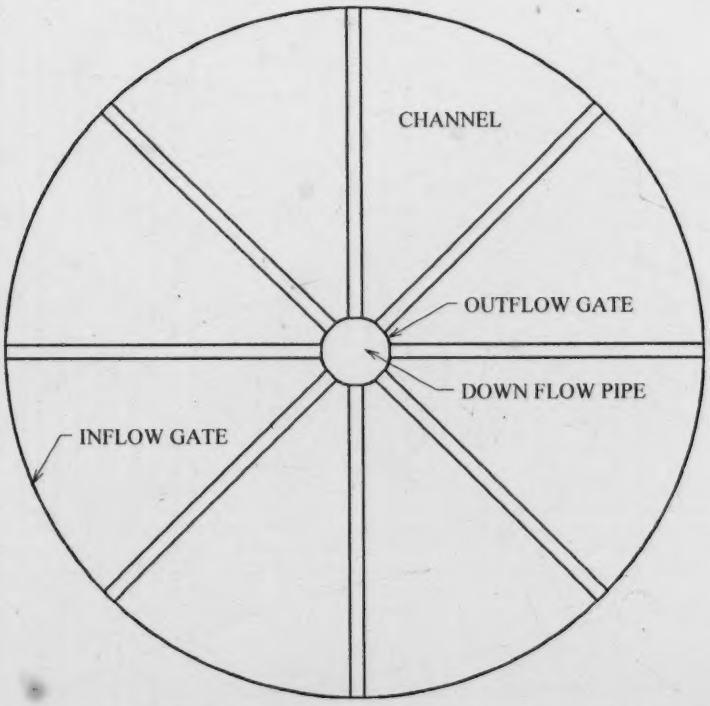

Figure 2.4.1: Conceptual design of the ocean based structure (overhead view).

The operational cycle of each modular channel can be divided into three phaese: the filling phase, the growth phase, and the draining phase. The filling phase begins when the channel is lowered by the ballast tanks, the inflow gate is lifted and water begins filling into the channel. During the filling phase any necessary nutrients are added and the growth phase begins as the filling phase ends when the inflow gate closes and the ballast tanks return the channel to its neutrally buoyant position. During the growth phase the microalgae grow until an essential limiting nutrient is depleted. Once the growth phase ends, the draining phase begins when the outflow

gate opens and the microalgae culture drains into the central section for disposal into the deep ocean (see Chapter 3 for more details on deep ocean disposal). During the draining phase not all of the culture is drained from the channel and the culture that remains is used as the inoculum for the next growth phase. Once the draining phase ends when the outflow gate closes the filling phase begins and the cycle repeats itself.

Each channel is required to be able to operate independently of the other channels since only one channel would drain at a time into the central section and thus into the down flow pipe. This allows for the diameter of the pipe to be minimized. In order to ensure that there is nearly continuous flow in the down flow pipe, the modular channels should consecutively empty into the central section, that is, when once channel finishes emptying the next channel in sequence should begin emptying. The number of channels necessary to ensure that the down flow pipe is operating continuously depends on the time of the filling, growth, and draining phase. The optimal number of channels can be determined from the following formula:

$$n = \frac{t_g - t_f}{t_d} + 1 \qquad \text{(Eq. 2.4.1)}$$

Where:

n: number of channels

t_g: time of growth phase

t_f: time of filling phase

t_d: time of draining phase

One of the most significant factors which could render an ocean based system unfeasible is its capital cost. While very little data is available in the literature

regarding the construction costs of VLFS, an attempt has been made to quantify the construction costs of five proposed MOB concepts constructed under different conditions (Bender, Blair, and Ayyub 2001). The MOB concepts reviewed were: steel rigidly connected semisubmersible, steel hinged semisubmersible, steel independent or dynamically positioned semisubmersible, flexible bridges between semisubmersible, and concrete and steel semisubmersible. Cost estimates were done for two construction scenarios, an afloat assembly scenario and a terrestrial assembly scenario, for each of these systems except for the steel independent or dynamically positioned semisubmersible where only the terrestrial assembly scenario was done. The cost per square meter for these systems was estimated to range from \$16,551 m^{-2} to \$35,142 m^{-2} with an average cost of \$24,316 m^{-2} (in US dollars).

To determine the cost of sequestering carbon using an ocean based system, the capital recovery factor was determined based on the estimates of the construction cost of the MOB. Three different construction costs of the MOB were used in this analysis: the maximum cost (\$35,142 m^{-2}), the average cost (\$24,316 m^{-2}) and the lowest cost (\$16,551 m^{-2}). Because this is a project of social interest a discount rate of 6.0% was selected. Fifty years was selected as the life of the project. Three different microalgal growth rates (on a dry weight basis) were used for this analysis: 1 g m^{-2} d^{-1} (a high rate for unmixed ponds), 10 g m^{-2} d^{-1}, and 40 g m^{-2} d^{-1} (the maximum rate achieved in raceway ponds). As noted in Chapter 1, the carbon content of microalgal biomass is about 50 wt%. Table 2.4.1 shows the annual cost per tonne of carbon dioxide sequestered based only on capital costs for the nine scenarios analyzed. The annual cost per tonne of carbon dioxide sequestered ranged from \$191,051 to \$20,222,643 per tonne of CO_2 with the actual cost likely being in the higher end of this range since lower microalgal grow are expected for an unmixed pond system. The construction costs make an ocean based system unfeasible since other methods for sequestering atmospheric carbon dioxide are at least three to five orders of magnitude less expensive. For example, the cost of

capturing carbon dioxide from a coal generated power plant and disposing it into the deep ocean has been estimated to cost between $90 and $180 per tonne of CO_2 (Fujioka et al. 1997). In order for an ocean based system to be competitive with other methods of carbon dioxide sequestration the construction costs would have to decrease by 3 to 5 orders of magnitude.

Based on this preliminary screening of the cost of ocean based systems, we discarded this option from further consideration.

Table 2.4.1: Annual cost per tonne of CO_2 sequestered based on the capital cost of an ocean based structure for three microalgal grow rates.

Cost per Area ($\$ m^{-2}$)	Annual Payment ($\$ m^{-2}$)	Microalgal Growth Rate ($g m^{-2} d^{-1}$)	Annual Mass of Carbon Dioxide Sequestered ($g m^{-2}$)	Annual Cost of Carbon Dioxide Sequestration ($\$ t^{-1}$)
175,194	11,115	1	550	20,222,643
		10	5496	2,022,264
		40	21985	505,566
111,075	7,047	1	550	12,821,443
		10	5496	1,282,144
		40	21985	320,536
66,205	4,200	1	550	7,642,050
		10	5496	764,205
		40	21985	191,051

2.4.3 Land Based System at Very Near Sea Level

A land based system operated at very near to sea level would be a series of large unmixed ponds constructed at approximately sea level adjacent to the ocean. Like an ocean based system, the advantage of having a land based system at sea level is that the distance that the ocean water is pumped to the system is minimized. The use of a pump can be eliminated if the pond is filled using a system of gates and the ocean tide.

A land based system operated at very near to sea level would be constructed of earth bermed or concrete walls protected against erosion during ocean storms, with the wall perpendicular to the direction of the ocean tide containing a series of vertically opening gates. This design would effectively create a lagoon separated from the ocean by the bermed walls. The inlet gate would be located at the midway point between low and high tide and would fill the pond at times when the tide is higher than the average tide (see Figure 3.4.2). The height of the seaward wall would have to exceed the height of high tide in order to prevent water from spilling over the top of the wall and into the ponds.

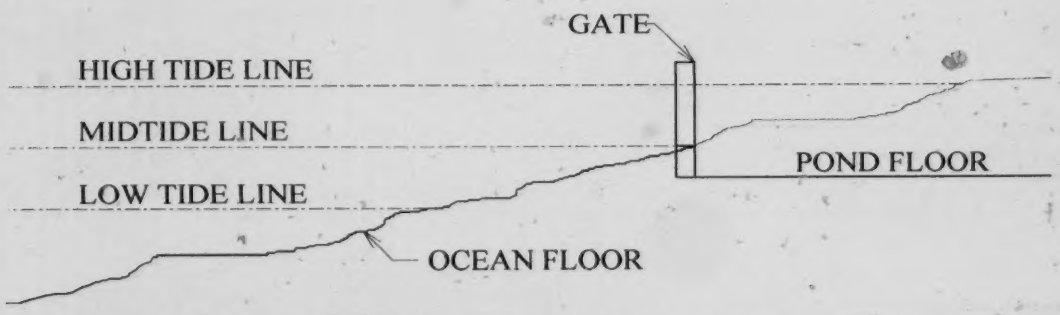

Figure 2.4.2: Location of inlet gate relative to tide level for the land based system at very near sea level.

The operational cycle of the land based pond system at near sea level, similar to ocean based system, consists of three phases: the filling phase, the growth phase, and the draining phase. The filling phase begins when the gates are opened and lasts until the pond is filled to a desired depth. Once the desired pond depth is achieved the gates close and the growth phase begins and lasts until the microalgae stop growing due to nutrient depletion. Once the growth phase ends, the draining phase begins. Not all of the culture is drained during the draining phase and the remaining culture is used as the inoculum for the next growth phase. Once the draining phase is complete, the gates open beginning the filling phase and the cycle repeats. Two options will be considered and discussed further below in this section for the draining phase that differ in where the culture is removed to from the pond

after the growth phase. The first option, the total discharge disposal system, removes the culture directly to the deep ocean from the ponds and the second option, the concentration disposal system, removes the culture to a ship for deep ocean disposal.

The total discharge system uses a series of pipes with one end connected to the discharge channel of the facility and the other emptying into the deep ocean (see Chapter 3 for more details on deep ocean disposal). One limitation of this system is the length of pipe required to connect the pond with the deep ocean which is determined largely in part by the width of the continental shelf. For example, off the west coast of Australia a pipe approximately 95 km long would be required to reach the deep ocean (see Figure 2.3.3b).

The concentration disposal option requires that the culture be pumped out of the ponds to a ship. Once the culture is loaded onto the ship, it would travel to a location on the ocean surface above the deep ocean and dispose of the culture into the deep ocean (again, see Chapter 3 for more details on deep ocean disposal). However, in order to increase the amount of carbon carried by the ship per voyage, the culture would likely be concentrated first. Therefore the pond culture would be pumped to a concentration system from the ponds before being pumped to the ship. A number of options exist for concentrating microalgae including centrifugation, sedimentation flotation, and filtration. A centrifugation system would most likely be used for this system since it is most suitable for the microalgal species *Dunaliella* and no chemicals would need to be added. While the concentrated microalgal mixture is sent to a ship for transport, the remaining microalgae free water can be disposed of back into the ocean surface water. Since the water that is rejected back to the ocean surface is reduced in carbon, the difference in the partial pressure of carbon dioxide between the atmosphere and the ocean surface water would increase. This would result in an increase in carbon dioxide flux from the atmosphere to the ocean surface. The limitations of this option include the cost of operating pumps to

transport the culture to the concentration system and to the ship, the capital and operating costs of the concentration system, and the cost of transporting the microalgae via ship to the deep ocean.

While both options for removing the culture from the ponds for the land based system operating at very near sea level have limitations, so does the system in its entirety. One of the biggest limitations of constructing this system is the scarcity of large areas of nearly flat land available at near ocean level and adjacent to the ocean, other than those containing a large human population. Practically, therefore, in order to construct this system a large quantity of earth would have to be removed in order to make the terrain ideal.

2.4.4 Land Based System above Sea Level

A land based system above sea level is similar to the system operated at sea level except for the method in which it is filled with ocean water. The land based system above sea level consists of a series of large unmixed ponds which use earthed bermed or concrete walls to contain the water. The water in the ponds is pumped up from the ocean. Figure 2.4.3 shows a conceptual design of the land based system above sea level.

The land based system above sea level also has the same three phase operational cycle as the two other system designs: the filling phase, the growth phase, and the draining phase. The filling phase begins when the filling pumps are activated and ocean water starts pumping into the ponds. Once the depth of the ponds reach a satisfactory level, the filling pumps are shut down and the growth phase begins. The growth phase continues until an essential nutrient is depleted and the draining phase begins. Similar to the land based system at very near sea level, two options exist for the removing the water during the draining phase. The two options for the draining phase, again, are to remove the culture directly to the deep ocean via pipeline (the total discharge disposal system) or to concentrate the culture and

remove it to a ship (the concentration disposal system). Each of these options has their limitations; direct disposal of the culture into the deep ocean requires a pipeline with a length that depends on location. For a western Australian location the pipeline length would be approximately 95 km. Removing the culture to a ship has costs of concentrating the culture and transporting it to the deep ocean via ship.

Since this land based system is above sea level the culture can be gravity drained to remove it from the ponds regardless of whether it is being sent directly to the deep ocean or if it is first being concentrated then sent to a ship. The advantages of being able to gravity drain the culture out of the ponds is that no power is required for pumping and power can be generated by installing a water turbine in the outflow pipes. This scheme is similar to that used for pumped storage of electricity where water is pumped up to an higher altitude reservoir during periods of low electricity demand and gravity drained through a water turbine to a lower reservoir to produce electricity during periods of high electricity demand. The efficiency of a modern pumped storage system is approximately 80% due to energy conversion losses suffered from the machinery (pump and turbine) and water losses due to evaporation in the upper reservoir which results in less water flowing through the turbine than was pumped up (Figueiredo, Flynn, and Cabral 2006). Assuming the energy recovery of the land based system above sea level is similar to that of a pumped storage system, 20% of the energy needed to pump the water from the ocean to the ponds would have come from an external source.

Note that it would be possible to operate a microalgal land based system above sea level in a manner to try to time the generation and consumption of electricity to gain value from the diurnal variation in power price (see, for example, Li and Flynn 2003). Ponds would be drained during periods of high power price, e.g. mid day and early evening, and filled during periods of low power price, e.g. midnight to 7 AM.

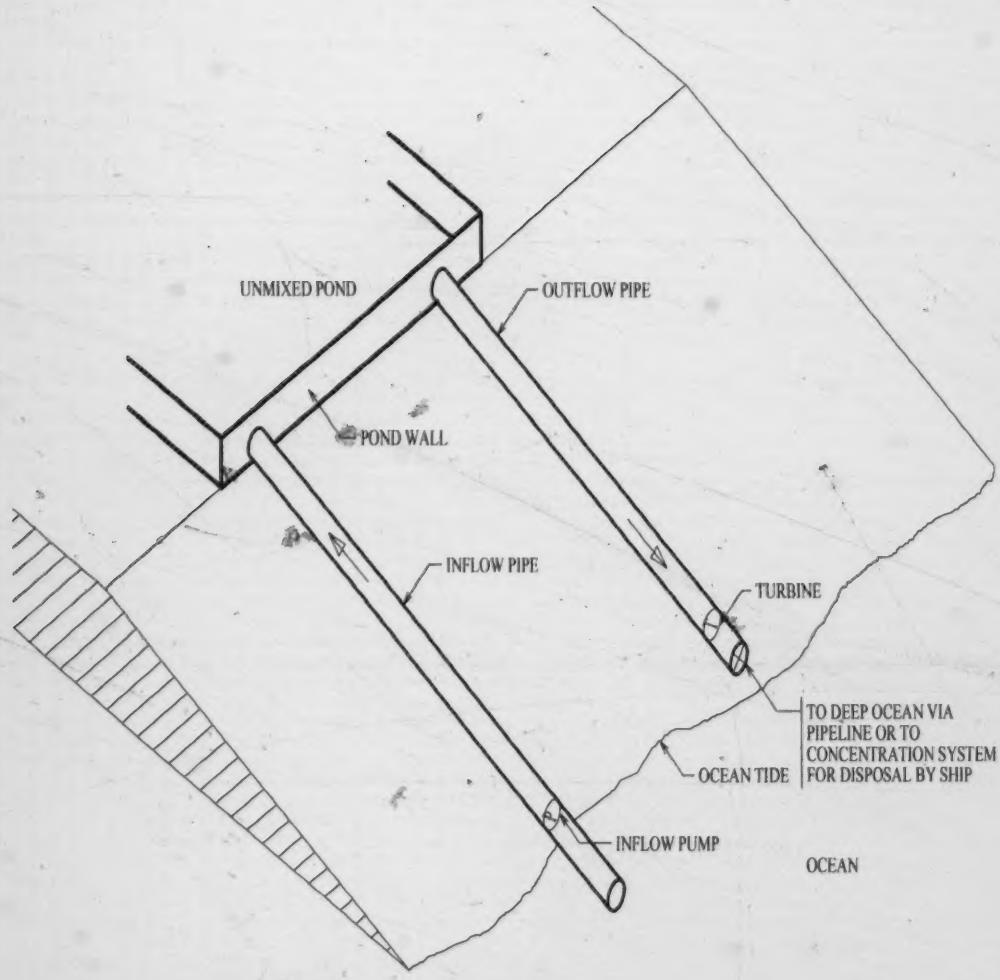

Figure 2.4.3: Conceptual design of the land based system above sea level.

2.4.5 Selection of Microalgal Carbon Dioxide Capture and Storage System Design

Ideally, the microalgal carbon dioxide capture and storage system would be at a very close proximity to the ocean (either on the ocean surface or adjacent to it on coastline) in order to minimize the amount of energy required for supplying ocean water used for microalgal growth and for the disposal of the microalgae in the deep ocean. While the ocean based system and the land based system at near ocean level

are close in proximity to the ocean, one is unfeasible and the other is unlikely. As noted above, the ocean based system is not feasible because of its high construction costs. The land based system at very near sea level is unlikely because of limited availability of unoccupied nearly flat land at near ocean level and adjacent to the ocean. Therefore the only system design that is practical in the near term is the land based system above sea level, and this system was selected as the design basis for this thesis. The economic feasibility of this system will be further investigated in Chapter 5.

For a land based system above sea level, pond water is discharged through a turbine to generate power, returning pond water to near sea level. Hence in Chapter 3 concepts of deep ocean disposal will be explored for the land based system at very near sea level, since both land based systems at very near sea level and above sea level discharge water into the deep ocean from the same approximate elevation. Note that rising ocean levels have the potential to create land areas near sea level that would be suitable for future microalgal production. For example, if rising sea levels were to flood portions of southern Florida, this shallow area could be bermed or walled to form microalgal ponds. There is little prospect of this occurring over the next 50 years since the rate of sea level rise is so low. If sea level rise where to remain constant at 3.1 mm yr^{-1} (Solomon et al. 2007), the average sea level rise would only be 0.16 m over the next 50 years.

2.5 Chapter Summary

All of the options selected for the microalgal carbon dioxide capture and storage system, as described in the previous sections of this chapter that were selected for this thesis are summarized in Figure 2.5.1.

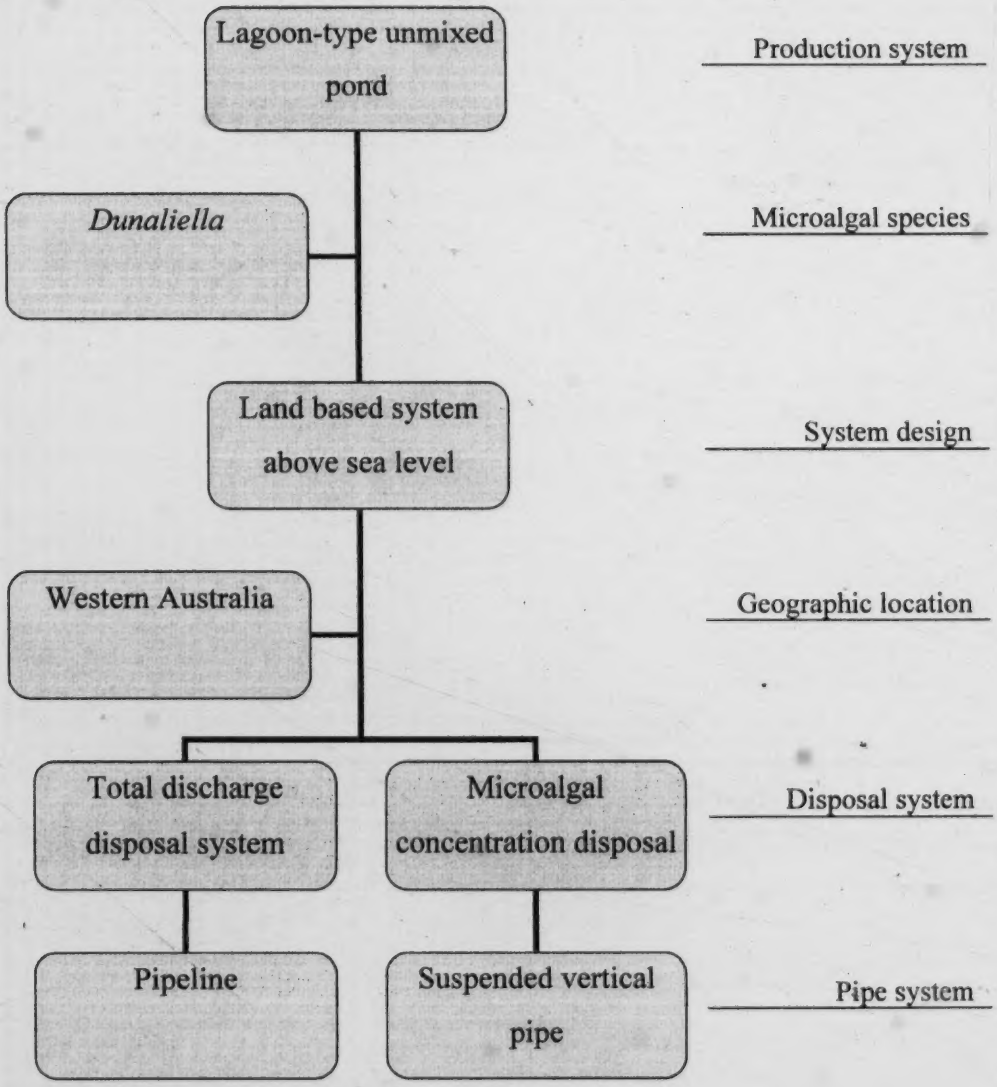

Figure 2.5.1: Summary of the microalgal atmospheric carbon dioxide capture and storage design options selected in Chapter 2.

Chapter 3

Deep Ocean Disposal

3.1 Introduction

The deep ocean is a suitable location for the long term storage of carbon captured from the atmosphere since it is isolated from the ocean surface by the pycnocline (as described in Chapter 1). While the pycnocline acts as a barrier between the upper and deep ocean, organic matter can sink from the upper ocean to the deep ocean. However, the amount of organic matter that reaches the deep ocean from the upper ocean is limited by biological processes.

Generally, dead microalgae sink in the ocean as marine snow (also known as biological rain, referring to all falling organic matter in the ocean comprised of dead animals or plants and fecal matter) at rates between 16 and 368 m d^{-1} (Turner 2002). At such rates it would take dead microalgae from a couple of days to a couple of months to sink to the deep ocean. However, only a small amount of dead organic matter (including microalgae) and therefore the organic carbon contained within the organic matter reach the deep ocean. The flux of organic carbon to the deep ocean is only approximately 1% (0.34 Gt yr^{-1}) of global marine primary production (Treguer et al. 2003). The flux of organic carbon to the deep ocean is small because of nutrient recycling, the process whereby some of the energy and nutrients in dead organic matter are reused by bacteria and other decomposers which ultimately releases the nutrients back into the ocean water.

The euphotic zone of the ocean is the upper layer where light penetrates the water. It rarely extends deeper than 100 m but can be as shallow as 5 to 10 m in coastal waters (Segar 1998). Since primary production (the production of organic compounds by photosynthesis minus the organic compounds used in respiration by

phototrophic organisms) occurs in the euphotic zone of the ocean, the majority of the nutrient recycling in the ocean occurs here as well. When microalgae die or are eaten by grazers and excreted as fecal matter the dead microalgae and fecal matter sink through the euphotic zone and are decomposed by decomposers such as bacteria. As the decomposers extract energy from the detritus, organic carbon contained in the microalgae is re-released in the euphotic zone where it can be reused in photosynthesis or it can escape to the atmosphere.

Because organic carbon is recycled in the euphotic zone, very little carbon is transferred from the upper layer of the ocean to the deep ocean. Therefore, in order to dispose of the carbon captured by microalgae from the atmosphere into the deep ocean, it is necessary to transport the microalgae directly to the deep ocean. Deep ocean disposal of microalgae can be done by transporting it in a down flow pipe which directly connects the surface to the deep ocean (see Section 3.2 for more details). In order to ensure that microalgae remains in the deep ocean once it has been transported there through the pipe, the density of the water in the pipe must be equal or greater than the density of deep ocean water. The density difference between the water in the pipe and the water of the ocean outside the pipe can also be used to drive the flow in the pipe from the surface to the deep ocean without mechanical pumping (see Section 3.3 for more details).

3.2 Down Flow Pipe

3.2.1 Overview

In general, the down flow pipe is a water pipe of sufficient length to connect the ocean surface to the deep ocean. The design of the down flow pipe used to dispose the microalgae into the deep ocean varies depending on the where it connects to the surface, that is whether the microalgae is sent directly to the deep ocean or whether it is disposed of by ship after having been concentrated. If the microalgae are sent directly to the deep ocean from the microalgal growth system, a pipeline is required

to connect the growth system near the coast to the deep ocean (see Section 3.2.2 for more details). If the microalgae are first concentrated then transported by ship for deep ocean disposal, a suspended vertical pipe is required to connect either the ship or an ocean structure to the deep ocean (see Section 3.2.3 for more details). The diameter of the pipes for either system depends on a number of factors including the material of the pipe, the length of the pipe and the flow rate within the pipe (see Section 3.3.2 for more details).

3.2.2 Pipeline

Because of the width of the continental shelf, the distance to the deep ocean from the coast of Western Australia is approximately 95 km (see Figure 2.3.3b. Because of this distance, an under water pipeline is required to connect the microalgal growth ponds to the deep ocean. The design and construction of such a pipeline is similar to existing ocean water pipelines. For example, a seawater supply pipeline exists off the coast of Hawaii which delivers cold ocean water used for aquaculture and ocean energy systems. The pipeline consists of over 3000 m of 1.4 m diameter pipe that reaches a depth of over 900 m (Makai Ocean Engineering 2007). The polyethylene pipe is anchored to the ocean floor where the topography is smooth and the pipe is suspended above the ocean when the topography is too rough. Concrete and fiberglass-reinforced plastic (FRP) pipelines of over 2400 m have also been constructed for ocean thermal energy conversion (OTEC) systems (Avery and Wu 1994). The concrete pipes had a diameter of up to 7.5 m and the FRP pipes had a diameter of up to 10 m, and were laid on the ocean floor.

3.2.3 Suspended Vertical Pipe

Two options exist for disposing the microalgae into the deep ocean by ship: through a suspended vertical pipe connected directly to the ship or by transporting the microalgae to a permanent floating ocean structure for disposal. A ship with the pipe connected directly to it would be similar in design to a drillship used for

offshore oil exploration. A drillship is ship shaped vessel equipped with drilling equipment such as a derrick and riser system used for drilling and extracting oil from below the ocean floor. The ship used for microalgae disposal would also be equipped with a derrick used to lower and a raise a segmented pipe into and out of the deep ocean. When not in use, the pipe segments would be stored on the ship deck, similar to the riser on a drillship. The ship would also have to be equipped with storage tanks to store the microalgae while the ship is in transit.

If the ship used to transport the microalgae were not equipped with a pipe, the ship would have to transport the microalgae to an ocean platform equipped with a suspended vertical pipe. The ship would have to be equipped with storage tanks in order to store the microalgae and a pumping system to deliver the microalgae to the disposal platform. The floating platform would be of similar design to a semi-submersible offshore oil platform. The platform would be equipped with a telescopic pipe and a derrick to operate the pipe. Alternatively, the pipe could remain lowered into the deep ocean permanently once it was first constructed, and lifted only when the structure had to return to a dock.

Regardless of whether the down flow pipe is attached to a ship or a platform, bending moments caused by the motion of the sea require that a pivoted connection be used to attach the pipe to the ship or platform. Flexible connections should also be used to connect subsequent sections of the pipe to limit any bending moments caused by subsurface currents which generally vary with depth.

A number of options for the material of the vertical pipe exist including steel, FRP, and lightweight concrete. In offshore oil recovery production risers have a fixed connection at both ends: the well head and the platform. Risers are generally pipes constructed of carbon steel. The diameter of these pipes depends on the depth to which they reach: a 0.4 m diameter pipe can be used for depths of just over a 1000 m and a 0.25 m diameter pipe can be used for depths of just over 2000 m

(Chakrabarti 2005). Other materials have been proposed for pipes such as titanium and composites, however they are generally considered to be too expensive.

In OTEC applications with a suspended pipe (as opposed to a pipeline laid on the ocean floor) one end of the pipe is freestanding. Fiberglass-reinforced plastic and lightweight concrete have been used to construct suspended pipes for OTEC applications. Fiberglass-reinforced plastic pipes have been constructed with diameters of up to 2.5 m and lightweight concrete pipes have been constructed with diameters of up to 3 m. Use of FRP and lightweight concrete pipes with diameters of up 10 m are deemed feasible in suspended applications (Avery and Wu 1994), and as noted above these diameters have been used in subsea pipes supported on the ocean floor.

3.3 Density Driven Flow

3.3.1 Overview

Fluids of different density can be distributed vertically based on their densities, forming stratified layers. Gravity is the driving force behind the stratification of fluids with different densities. Gravity causes more dense fluids to sink through less dense fluids and less dense fluids to rise through more dense fluids. Since a fluid of greater density will sink when placed on top of a fluid of lesser density, flow down the pipe into the deep ocean can be produced if the density of water being sent down the pipe is greater than the density of the ocean column outside the pipe.

In order to successfully flow the microalgal culture down a pipe into the deep ocean using the density gradient between the pond culture water and the deep ocean water, a number of factors need to be considered and are discussed in the four subsequent sections. Section 3.3.2 describes the relationship between temperature, salinity, and density and how a sufficient pond water density is achieved to produce flow in the down flow pipe. Section 3.3.3 describes the vertical density profile of the ocean and

how the density gradient between the higher density pond water and the lower density ocean water is the driving force behind the flow in the pipe. In Section 3.3.4 hydrostatic head and friction head of the pipe system are discussed. In Section 3.3.5 the relationship between pond depth and pond water density are discussed.

3.3.2 Temperature, Salinity, and Density

The density of pure liquid water at 4°C and 1 atmosphere is 1000 kg m^{-3} and varies as temperature, salinity and pressure change. The density of water increases as salinity and pressure increase and decreases as temperature increases. Since water is almost incompressible, changes in pressure have a very small effect on density; the density of ocean water at the deepest depths is only about 2% greater than at the surface due to pressure effects (Segar 1998). That is, two parcels of water with identical properties would only vary in density by about 2% if one were at the ocean surface and the other at the deepest depths of the ocean.

Pressure effects can be ignored in considering the flow of water down a pipe into the deep ocean, because the increase in pressure with depth is essentially the same inside and outside the pipe. Thus, at a given salinity and temperature the density of the ocean water will increase slightly with depth, but so to will the density of the water in the pipe. The effects offset one another.

The relationship between temperature, salinity, and density for seawater is given by the international one-atmosphere equation of state for salinities from 0.5 to 43 practical salinity units as described by Millero and Poisson (1981). Poisson and Gadhoumi (1993) further extend this equation of state to include salinities up to 50 PSU. The PSU is a unit based on the ratio of electrical conductivity of sea water to that of a standard concentration of potassium chloride solution and is approximately equal to parts per thousand. Note that in previous literature the practical salinity unit was used as the unit of salinity; however more modern convention is to consider salinity to be dimensionless. Figure 3.3.1 shows curves of density as a

function of temperature for different salinities of water calculated using the equation of state (see Appendix A for further details). Note that the density calculated is for sea water at one atmosphere of pressure, i.e. the pressure effect on density is not calculated.

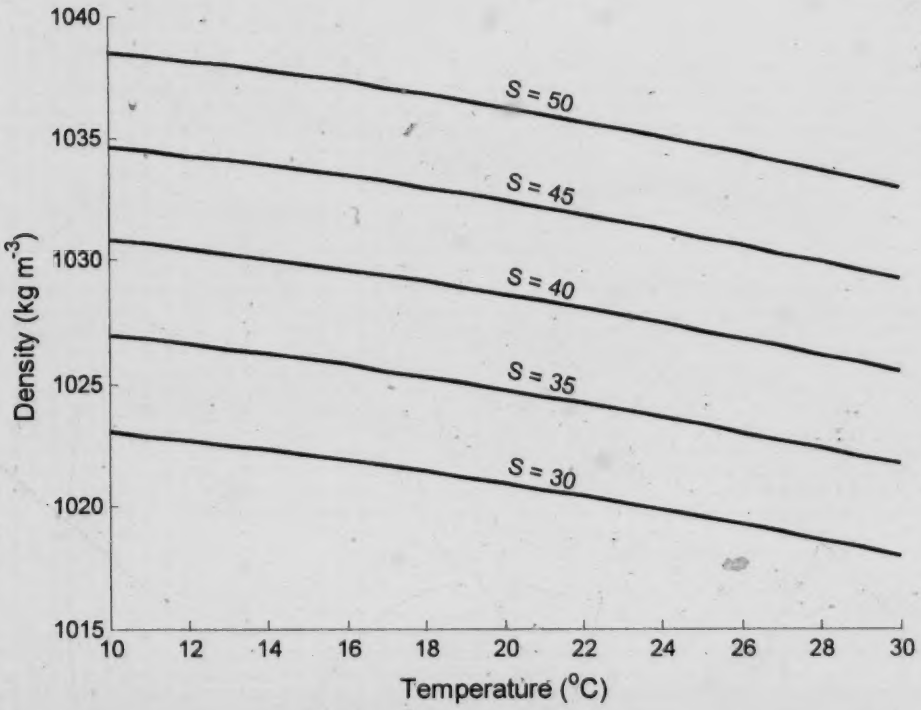

Figure 3.3.1: Density as a function of temperature for salinities ranging from 30 to 50 PSU calculated using the equation of state (Millero and Poisson 1981; Poisson and Gadhoumi 1993).

In order to achieve a sufficiently high density in the pond water to produce flow down the pipe, the salinity of the pond water must be increased. The salinity of pond water can be increased by solar evaporation; as water in the pond is lost due to evaporation, the relative concentration of salts increases and hence salinity increases. Once evaporation has increased the salinity of the pond water so that its density is sufficiently high, the microalgal culture can then be sent down the down

flow pipe driven by the density gradient. Values of density for ocean water will be discussed in Section 3.3.3 and rates of evaporation will be discussed in Section 3.3.6.

Water in a shallow pond exposed to high solar radiation will warm. Because increasing temperatures decrease the density of water, a sufficiently high design temperature of the pond water needs to be specified, in order to ensure that the increase in density due to salinity is sufficient, and in particular that it more than offsets the decrease in density due to increased temperature. The pond water design temperature in this study was set at 30°C which is close to maximum mean ambient maximum temperature for the location selected in Western Australia (see Section 2.3.2). Note that pond water design temperature would need to be verified by further analysis if an actual design were to proceed.

3.3.3 Ocean Density Profile and Density Gradient

As previously discussed in Chapter 1, the density of the ocean increases with depth in a nonlinear manner due to changes in temperature and salinity. Figure 3.3.2 shows the temperature and salinity depth profile for a location off the coast of Western Australia at 29.2°S, 113.1°E which were constructed using data from a temperature/salinity profiling float (float ID 5900785, profile date December 15, 2004) launched as part of the International Argo Project obtained from the National Oceanographic Data Center (USDOC 2007). Using the temperature and salinity data, the density depth profile can be calculated using the equation of state and is shown in Figure 3.3.3. (Note again that the density shown in Figure 3.3.3 is at a pressure of one atmosphere, and hence is not the actual density at depth. The density at depth would be higher than the calculated value, but the density at depth of a unit of water descending a pipe into the deep ocean would increase to the same extent, as noted above.) From Figure 3.3.3 it can be seen that the pycnocline extends to a depth of approximately 800 m as primarily determined by the decrease in temperature, and at depths deeper than this, density is relatively constant, with changes arising from slight changes in salinity with depth.

The density of the pond water must satisfy two conditions: it must be great enough to cause flow down the pipe, and it must be equal to or greater than the density of the ocean water at the point of discharge. If the density of the pond water were less than the density of the ocean water at the point of discharge, the water exiting the pipe would rise through the ocean column and risk being exposed to mixing in the shallow ocean. If the water exiting the pipe returns to shallow ocean the subsequent decay of the microalgae (in the euphotic zone) would release carbon dioxide back to the shallow ocean and ultimately to the atmosphere. If we assume that heat transfer across the pipe wall from the pond water to the ocean is negligible, we can see from Figure 3.3.3 that the density of the pond water and thus the density of the water in the down flow pipe must at a minimum be at least equal to approximately 1027.3 kg m^{-3} and the down flow pipe must extend to a depth of greater than 800 m.

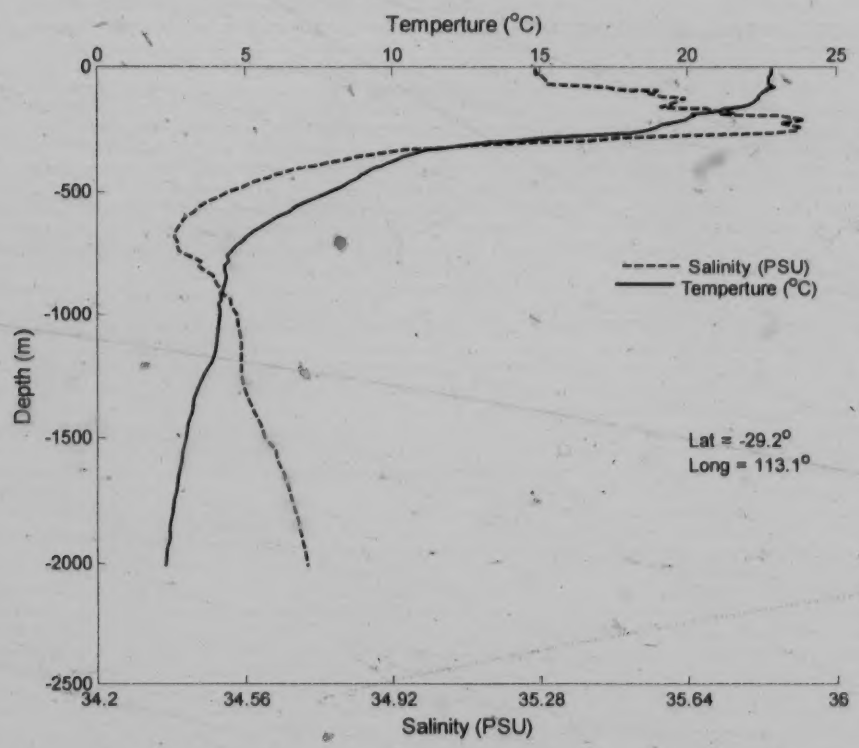

Figure 3.3.2: Ocean water temperature and salinity depth profile at 29.2°S, 113.1°E; plot produced from data from USDOC (2007).

A plot of density as a function of depth for the ocean water and for the water in the pipe is shown in Figure 3.3.4. The higher density of the water inside the pipe helps create a higher hydrostatic pressure inside the pipe compared to the ocean water column. A sufficient hydrostatic pressure difference between the water inside the pipe and the ocean water column will produce flow inside the pipe (see Section 3.3.4 for more details).

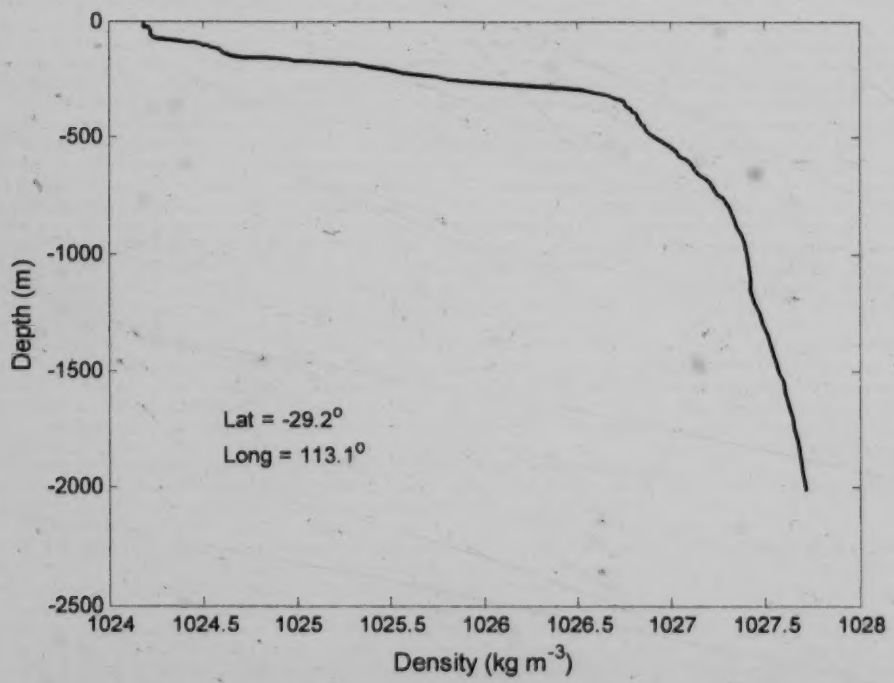

Figure 3.3.3: Ocean water density depth profile (adjusted to one atmosphere pressure) at 29.2°S, 113.1°E calculated using the international one-atmosphere equation of state of seawater; plot produced from data from USDOC (2007).

Note that heat transfer from the warmer water inside the pipe through the pipe wall to the colder outside water lowers the temperature of the water inside the pipe and thus its density. However, given the large diameter of the pipe and hence the low

relative surface area for heat transfer relative to the volume of flow, this effect is ignored in this thesis.

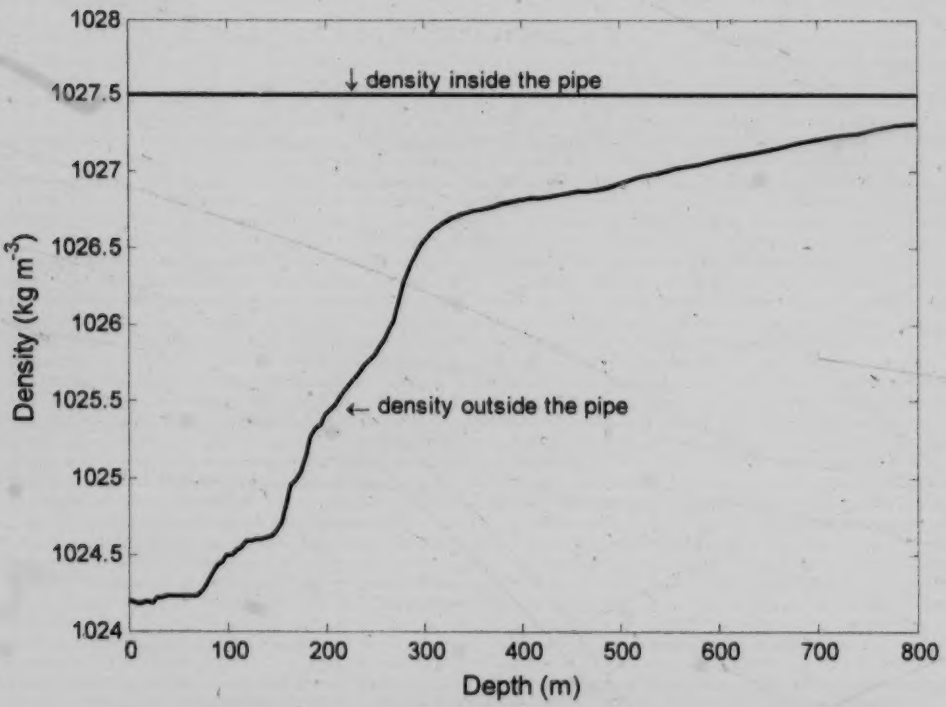

Figure 3.3.4: Density (adjusted to one atmosphere pressure) as a function of depth for the water inside the pipe and the ocean water column outside the pipe.

3.3.4 Hydrostatic Head

A pressure gradient occurs when there is a difference in hydrostatic pressure caused by a difference in elevation, a difference in densities or a combination of both between the surfaces of two connected reservoirs. For example, in Figure 3.3.5 if the liquids in each of the reservoirs are of different density and do not mix at the interface, then the hydrostatic pressure that each liquid exerts on the other is given by the following formula:

$p_s = \rho g h$ (Eq. 3.3.1)

Where:

p_s: hydrostatic pressure

ρ: density of the liquid

g: acceleration due to gravity

h: elevation

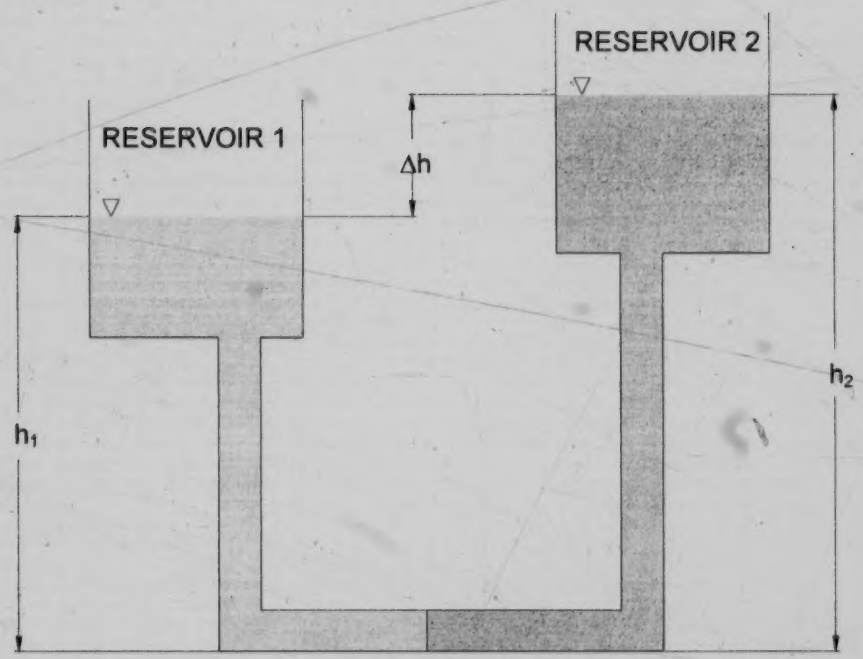

Figure 3.3.5: Two reservoir system where fluid 1 is in reservoir 1 and fluid 2 is in reservoir 2. The fluids meet at the interface.

The net hydrostatic pressure exerted on the liquids at the interface is found by subtracting the hydrostatic pressure cause by the liquid in reservoir 1 by the hydrostatic pressure caused by the liquid in reservoir 2:

$$\Delta p_s = p_{s1} - p_{s2} = \rho_1 g h_1 - \rho_2 g h_2 \qquad \text{(Eq. 3.3.2)}$$

Where:

Δp_s: hydrostatic pressure difference

p_{s1}: hydrostatic pressure of reservoir 1

p_{s2}: hydrostatic pressure of reservoir 2

ρ_1: density of fluid 1

ρ_2: density of fluid 2

$h1$: elevation of fluid surface 1

$h2$: elevation of fluid surface 2

g: acceleration due to gravity

If the resulting value of Equation 3.3.2 is positive then p_{s1} is greater than p_{s2} and the fluid flows from reservoir 1 to reservoir 2. If the resulting value of Equation 3.3.2 is negative than p_{s1} is less than p_{s2} and the fluid flows from reservoir 2 to reservoir 1. If the resulting value of Equation 3.3.2 is zero than p_{s1} is equal to p_{s2} and no flow occurs since the system is in hydrodynamic equilibrium.

If the densities of the fluids are the same in Figure 3.3.5 than Equation 3.3.2 reduces to:

$$\Delta p_s = \rho g(h_1 - h_2) = \rho g \Delta h \qquad \text{(Eq. 3.3.3)}$$

In Equation 3.3.3, the difference in elevation is known as hydrostatic head.

If the two liquids in Figure 3.3.5 were of the same density and the liquid from reservoir 1 were to be pumped into reservoir 2 the pump would have to produce enough pressure to overcome the hydrostatic pressure caused by the elevation difference.

For a reservoir where density is not constant with depth (such as the ocean) the hydrostatic pressure is found by integrating the liquid's density over the depth:

$$p_s = \int_{z_1}^{z_2} g\rho dz \qquad \text{(Eq. 3.3.4)}$$

In Equation 3.3.4 density is a function of vertical distance, 'z'.

In order to produce flow down the pipe the hydrostatic pressure of the water column inside the pipe must be greater than the hydrostatic pressure of the water column outside of the pipe. If the water level in the pipe is at a lower elevation than the ocean surface, the density of the water inside the pipe needs to be sufficiently high enough to overcome this elevation difference. The elevation differences for both of the systems being considered (the total discharge disposal system and the microalgal concentration system) are discussed in greater detain in Section 3.4.3.

The hydrostatic pressure of the water column also has to be sufficiently high enough to overcome frictional losses inside the pipe. Friction is further discussed in Section 3.3.5.

3.3.5 Friction

Friction losses in a pipe are caused by the friction between the fluid flowing in the pipe and the pipe wall. The head loss due to friction in a pipe can be found using the following equation:

$$h_f = f\frac{L}{d}\frac{V^2}{2g} \qquad \text{(Eq. 3.3.6)}$$

Where:

h_f: frictional head loss

f: Darcy friction factor

L: pipe length

d: pipe diameter

V: velocity of fluid in the pipe

g: acceleration due to gravity

The Darcy friction factor is a function of Reynolds number, pipe material, and pipe shape. As will be shown in Section 3.4, calculating the friction factor differs for laminar and turbulent flow.

3.3.6 Pond Depth and Density

As previously noted in Section 3.3.2, to achieve the necessary density in the microalgae ponds to drive flow in the pipe into the deep ocean, the salinity of the pond water must be increased through evaporation. The salinity of the ocean surface water off the coast of Western Australia, which is used as the growth medium, is approximately 35.8 practical salinity units (PSU) as shown in Figure 3.3.2 (salinity depth profile). The mean daily net evaporation in Western Australia averaged per month ranges from 0.03 mm per day to 10.6 mm per day with an annual daily mean of 5.5 mm per day. Based on the initial salinity of the growth pond water (35.8 PSU, that of the ocean surface water) and the rate of evaporation the time required to achieve a sufficiently high salinity so that density is able to drive flow down the pipe is set by the depth of the growth pond. A first order approximation relating salinity with pond depth and evaporation is given as follows:

$$S_f = S_i \frac{d_i}{d_i - Et} \qquad \text{(Eq. 3.3.7)}$$

Where:

S_f: final salinity (PSU)

S_i: initial salinity (PSU)

d_i: initial pond depth (m)

E: evaporation rate (m per day)

t: time (day)

Equation 3.3.7 is only a first order approximation since it assumes that the rate of evaporation is constant regardless of salinity when in reality the rate of evaporation decreases as salinity increases. However, this effect is ignored in this thesis.

Equation 3.3.7 will be used to evaluate the interaction between depth of the pond and the time required to achieve the desired salinity in order to produce flow in the down flow pipe in Section 3.4 once the required density is determined (again, see Section 3.4).

3.4 Required Pond Water Density

3.4.1 Overview

An analysis of the down flow pipe system connecting the microalgae disposal pond to the deep ocean is required to determine the necessary growth pond water density that is required in order to produce flow down the pipe. In order to determine the required density, the equations governing the system must be set up and the physical properties (such as pipe length and diameter) of the system must be defined as is done in Section 3.4.2. In Section 3.4.3, required densities are calculated for the total discharge disposal system and for the microalgal concentration system (via ship or floating platform). Once the required density is calculated, the time required to achieve this density can be calculated as a function of pond depth, which is investigated in Section 3.4.4.

3.4.2 Density Calculations

A list and brief description of the symbols used in this section is given in Table 3.4.1.

Table 3.4.1: List of symbols used in Section 3.4.2

Symbol	Description	Units	Symbol	Description	Units
D	pipe diameter	m	ρ_o	density outside the pipe	kg m^{-3}
f	friction factor	-	V	flow velocity	m s^{-1}
g	accelaration due to gravity	m s^{-2}	V_1	flow velocity at point 1	m s^{-1}
h_f	head loss due to pressure	m	V_2	flow velocity at point 2	m s^{-1}
L	pipe length	m	z	elevation	m
p_1	pressure at point 1	Pa	z_0	elevation at the ocean surface	m
p_2	pressure at point 2	Pa	z_1	elevation at point 1	m
p_f	pressure loss due to friction	Pa	z_2	elevation at point 2	m
Re_d	Reynolds number	-	ε	pipe roughness	m
ρ_i	density inside the pipe	kg m^{-3}	μ	viscosity	kg m^{-1} s^{-1}

Refer to Figure 3.4.1 for locations of points 1 and 2

The density of the water required in the pipe can be calculated by applying the energy equation along the length of the pipe from point 1 to point 2 (see Figure 3.4.1). The energy equation is as follows:

$$p_1 + \frac{V_1^2}{2}\rho_i + \rho_i g(z_2 - z_1) = p_2 + \frac{V_2^2}{2}\rho_i + g\int_{z_0}^{z_2}\rho_o dz + p_f \qquad \text{(Eq. 3.4.1)}$$

Equation 3.4.1 can be simplified since no pressure forces are applied to the system at points 1 and 2 other than by hydrostatic forces. Also, the velocity at the top of the pipe (point 1) is equal to the velocity at the pipe exit (point 2). Therefore Equation 3.4.1 can be rewritten as:

$$\rho_i g(z_2 - z_1) - g\int_{z_0}^{z_2}\rho_o dz = p_f \qquad \text{(Eq. 3.4.2)}$$

The right-hand side of Equation 3.4.2 is the hydrostatic head difference between points 1 and 2. If pressure loss due to friction is recalculated as head loss then Equation 3.4.2 becomes:

$$\rho_i g(z_2 - z_1) - g\int_{z_0}^{z_2} \rho_o dz = \rho_i g h_f \qquad \text{(Eq. 3.4.3)}$$

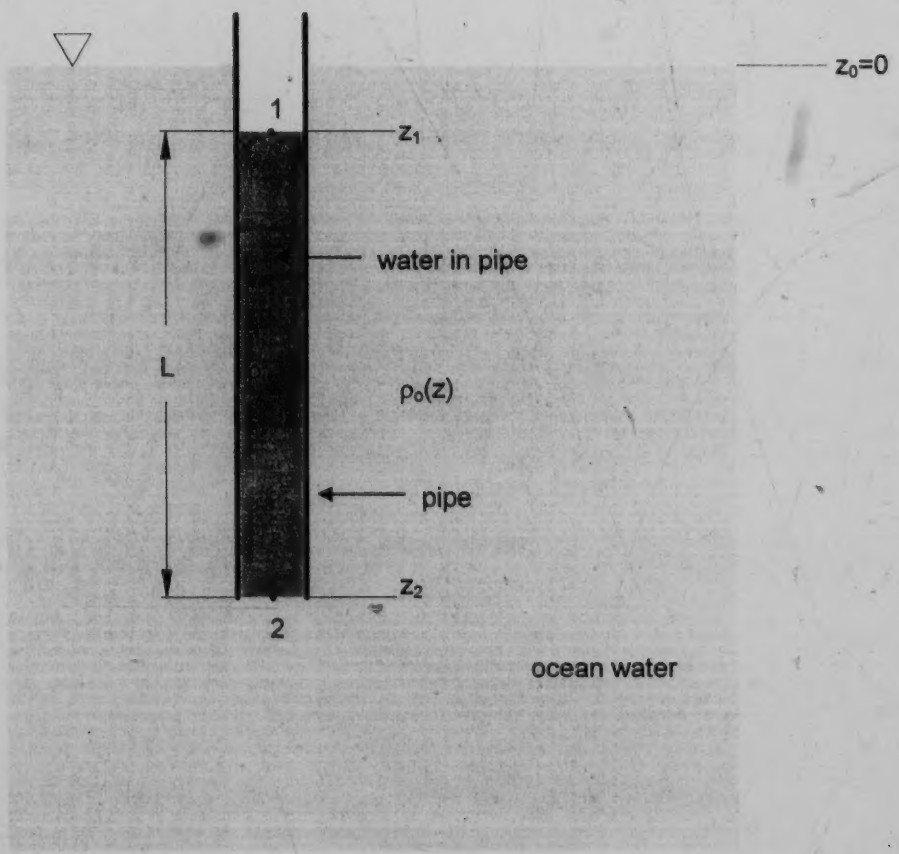

Figure 3.4.1: Conceptual Ocean disposal pipe system.

Equation 3.4.3 can be rearranged to solve for ρ_i:

$$\rho_i = \frac{\int_{z_0}^{z_2} \rho_o dz}{(z_2 - z_1) - h_f} \qquad \text{(Eq. 3.4.4)}$$

The integral in Equation 3.4.4 has to be solved using a numerical integration method since ρ_o is not given as a mathematical formula as a function of depth but rather as a series of data points corresponding to different depths. Because the data points for ρ_o were not measured at constant depth intervals, the Trapezoidal Rule with uneven segments was used to evaluate this integral. The Trapezoidal Rule is given as follows:

$$\int_a^b f(x)dx \approx (x_1 - x_0)\frac{f(x_0) + f(x_1)}{2} + (x_2 - x_1)\frac{f(x_1) + f(x_2)}{2} + \ldots + (x_n - x_{n-1})\frac{f(x_{n-1}) + f(x_n)}{2}$$

(Eq. 3.4.5)

In Equation 3.4.5, *f(x)* is some continuous function in *x* and the integral is evaluated from some lower limit *a* to some upper limit *b*. The term *n* represents the number of segments that the data is divided into.

In Equation 3.4.4, the friction head, h_f, can be solved for using Equation 3.3.6:

$$h_f = f\frac{L}{D}\frac{V^2}{2g} \qquad \text{(Eq. 3.3.6)}$$

Friction factor, *f*, in Equation 3.3.6 depends on whether flow in the pipe is laminar or turbulent, which is determined by the Reynolds number. The Reynolds number

is the ratio of inertial forces to viscous forces of the fluid flow. For flow in a round pipe, the Reynolds number is as follows:

$$\mathrm{Re}_d = \frac{\rho_i V D}{\mu} \qquad \text{(Eq. 3.4.6)}$$

Pipe flow is laminar for Reynolds numbers below 2300 and transitions to turbulent at Reynolds numbers greater than this. For laminar pipe flow, the friction factor can be found from the following formula:

$$f_{lam} = \frac{64}{\mathrm{Re}_d} \qquad \text{(Eq. 3.4.7)}$$

The friction factor for turbulent pipe flow can be approximated from the formula given by Haaland (1983):

$$\frac{1}{f^{1/2}} \approx -1.8 \log\left[\frac{6.9}{\mathrm{Re}_d} + \left(\frac{\varepsilon/D}{3.7}\right)^{1.11}\right] \qquad \text{(Eq. 3.4.8)}$$

In order to solve Equation 3.4.4 for the density inside the pipe, friction factor must be calculated. However, friction factor is a function of Reynolds number which is a function of the density inside the pipe. Therefore Equation 3.4.4 is an implicit relation which can be solved using an iterative approach. To solve Equation 3.4.4 iteratively, an initial guess of inside density is made in order to solve for friction factor which is then used to solve Equation 3.4.4. The density calculated from Equation 3.4.4 is then compared with the initial guess and if the difference of the two is within an acceptable tolerance, than density has been solved for. However, if the difference of the two densities is not within an acceptable tolerance, then the process has to be repeated using the calculated density as the next guess. This process continues until the difference of the calculated density and guessed density

are less than the acceptable tolerance. A tolerance of 10^{-6} kg m^{-3} was selected for these calculations.

The density inside the pipe was solved for using the equations and methods described above by writing MATLAB code that solved Equation 3.4.4 for density. Appendix B contains the MATLAB code and gives a brief description of it. A number of constants were defined to solve for density (such as pipe diameter, pipe roughness, flow velocity, and viscosity) and will be further discussed in Section 3.4.3.

3.4.3 Density Calculation Results

Density calculations were performed for two different systems using the methods described in Section 3.4.2: a pipeline system connected to the shore and a vertical pipe system connected to a floating platform. For both systems, 800m was selected for the disposal depth (z_2 equals 800 m in Figure 3.4.1). The desired flow velocity for both systems was set at 1.5 m s^{-1} and the dynamic viscosity of the water in the pipe was selected as 1.07×10^{-3} kg m^{-1} s^{-1} (which corresponds to a temperature of 20°C and a salinity of 35 PSU at 1 atm pressure) (White 2003). Dynamic viscosity varies with salinity and temperature and pressure; however these effects were deemed to be negligible since the variation is small. The viscosity of water decreases marginally at temperatures below 30°C and only changes by a few percent for pressures up 100 atm. Increasing the salinity of water from 0 PSU to 35 PSU (at 20°C and 1 atm) only increases viscosity by about 7% (White 2003).

For the total discharge disposal system and, a worst case was developed for the negative elevation difference between the disposal pipe and the ocean, as follows: assume that a pond near sea level is filled only when the ocean is above mean sea level, with an assumed head of 0.5 m between the ocean at mean sea level and the pond, i.e. the pond elevation is 0.5 m below mean sea level. Further, assume the pond is drained only when the ocean is below mean sea level, with an assumed head

of 0.5 m between the pond and the inlet to the pipe. Then the difference in the level of water in the disposal pipe from sea level, z_1 in Figure 3.4.1, is 1 m. Note that the assumption of the pond water discharge elevation being 1 m lower than sea level is the worst case, since for a land based system above sea level the discharge from the turbine outlet as the water returns from the pond to near sea level could be adjusted to be a few meters above sea level if required.

The required density of the water inside the pipe was calculated using a 7.5 m diameter concrete pipe with pipe roughness of 4.0×10^{-5} m (White 2003). The length of the pipeline was calculated by adding the horizontal distance (95,000 m) the pipeline needs to cover to the disposal depth (800 m). The internal density required for this system in order to produce flow down the pipeline is 1038.4 kg m^{-3} which corresponds to a salinity of 57.3 PSU; the flow regime is turbulent (Re_d 3.6×10^6). Note that this salinity is only an estimate since it was calculated using the equation of state of seawater which is only applicable for salinities up to 50 PSU. Since this value is greater than the density of the ocean at point of discharge, 1027.3 kg m^{-3}, it is the governing density for purposes of design. The parameters used to define this system and the required density are summarized in Table 3.4.2.

Table 3.4.2: Parameters used to calculate density for the pipeline disposal system.

Parameter	Value
Disposal depth, z_2 (m)	800
Pipe length, L (m)	95,799
Pipe diameter, D (m)	2.5
Pipe roughness, ε (m)	4.0×10^{-5}
Flow velocity, V (m s^{-1})	1.5
Reynolds number, Re_d	3.6×10^6
Density inside the pipe, ρ_1 (kg m^{-3})	1038.4
Salinity, S (PSU)	57.3

For the microalgal concentration system, the density of the water inside the pipe was calculated using a 2.5 m diameter fiberglass-reinforced plastic (FRP) pipe with a pipe roughness of 3.0×10^{-7} m (Mott 2006). As a worst case we assume that the level of water in the ship compartment is 1 m below the surface level of the ocean. The internal density required for this system in order to produce flow down the pipeline is 1027.6 kg m^{-3} which corresponds to a salinity of 42.1 PSU; the flow regime is turbulent (Re_d 3.6×10^6). Since this value is greater than the density of the ocean at point of discharge, 1027.3 kg m^{-3}, it is the governing density for purposes of design. The parameters used to define this system and the required density are summarized in Table 3.4.3.

Table 3.4.3: Parameters used to calculate density for the suspended vertical pipe disposal system.

Parameter	Value
Disposal depth, z_2 (m)	800
Pipe length, L (m)	799
Pipe diameter, D (m)	2.5
Pipe roughness, ε (m)	3.0×10^{-7}
Flow velocity, V (m s^{-1})	1.5
Reynolds number, Re_d	3.6×10^6
Density inside the pipe, ρ_i (kg m^{-3})	1027.6
Salinity, S (PSU)	42.1

3.4.4 Density, Salinity and Pond Depth Relationship

As previously discussed, in order to achieve the necessary density in the down flow pipe, the salinity of the microalgal pond water needs to be increased through solar evaporation in order to achieve this density. The time required to achieve the necessary salinity depends on the initial salinity (35.8 PSU, see Section 3.3.6), evaporation rate and can be calculated by rearranging Equation 3.3.7 to give:

$$t = \frac{d_i}{E}\left(1 - \frac{S_i}{S_f}\right) \qquad \text{(Eq. 3.4.9)}$$

Where:

S_f: final salinity (PSU)

S_i: initial salinity (PSU)

d_i: initial pond depth (m)

E: evaporation rate (m per day)

t: time (day)

The time required to reach the target density for the pipeline system and the suspended vertical pipe system were calculated using Equation 3.4.9 and the minimum monthly (0.03 mm d^{-1}), annual average (5.5 mm d^{-1}), and maximum monthly (10.6 mm d^{-1}) daily net evaporation rates. Table 3.4.4 shows the range of time required to achieve the target density for the pipeline system (1038.4 kg m^{-3}, corresponding to a salinity of 57.3 PSU) and the suspended vertical pipe system (1027.6 kg m^{-3}, corresponding to a salinity of 42.1 PSU).

Based on previous pond designs (see Section 2.2.2) and the precision to which these ponds can be constructed, the construction of a pond with a depth of 0.2 m is achievable and was selected as the pond depth for this thesis. Therefore design holdup for the average net evaporation rate in the ponds is 6 days for disposal by ship and 14 days for disposal by pipeline from shore to the deep ocean. However, net evaporation rates in Western Australia (see Table 2.3.1) are very low for the winter months, particularly June, July and August. For any depth of pond evaporation periods are excessive during this time. For the winter months, the time periods are so long that the microalgal ponds would likely be contaminated by predatory species if the microalgae were held in the pond for the entire time period. Table 3.4.4 shows evaporation periods of well over a year at the minimum net evaporation rate, which occurs in July. In August, the third lowest month for net

evaporation, periods of 28 and 69 days are required to achieve the target salinities for the ship and pipeline disposal options, respectively. Hence, for the three winter months the pond system might be closed or continue to operate by spiking the pond water discharge stream with a stream of previously made high saline water. This is discussed in Section 4.2.

Table 3.4.4: Time (in days) required to reach the target density based on daily net evaporation rates for the pipeline system and the suspended vertical pipe system. The daily net evaporation rates used are the minimum monthly (0.03 mm d^{-1}), annual average (5.5 mm d^{-1}), and maximum monthly (10.6 mm d^{-1}).

Initial Pond depth (m)	Evaporation Rate (mm d^{-1}) 0.03	5.5	10.6
Pipeline System (Target S = 57.3 PSU)			
0.1	1250.7	6.9	3.5
0.2	2501.5	13.7	7.1
0.3	3752.2	20.6	10.6
0.4	5002.9	27.5	14.1
0.5	6253.6	34.4	17.7
0.6	7504.4	41.2	21.2
Suspended Vertical Pipe (Target S = 42.1 PSU)			
0.1	498.8	2.7	1.4
0.2	997.6	5.5	2.8
0.3	1496.4	8.2	4.2
0.4	1995.2	11.0	5.6
0.5	2494.1	13.7	7.1
0.6	2992.9	16.4	8.5

Chapter 4

Limiting Factors

4.1 Introduction

During the operation of the microalgal atmospheric carbon dioxide capture and storage system, a number of simultaneous processes are occurring: the evaporation rate of the pond water in order to increase its salinity, the growth rate of the microalgae using incident light, and the diffusion of carbon dioxide from the atmosphere into the pond water. In this section we explore the rate limiting step and its consequences on the design of a microalgal atmospheric carbon sequestration system. The implicit assumption is that the hydraulic features of the pond filling and discharge systems can be designed so as not to be the rate limiting step.

4.2 Evaporation Rate

Based on a pond depth of 0.2 m, the average time required for sufficient evaporation to occur in order to increase the density of the pond water to produce flow is approximately 14 days for the pipeline system and approximately 6 days for the suspended vertical pipe system. If the rate of evaporation is limiting, or if pond retention times for evaporation are higher than the retention time required to deplete a limiting nutrient (discussed further in Section 4.4), then the pond system can be combined with an adjacent solar evaporation pond. The pond would be used to accumulate highly saline water which could be mixed with pond water as it flows into the discharge system. Note that in all months in Western Australia the net rate of evaporation is positive, so dilution of the solar evaporation pond water by net rainfall is not likely. Given the very high net evaporation rates in Western Australia in summer months, it would be easy to accumulate a reservoir of high salinity water.

4.3 Microalgal Growth Rate

Plant growth from photosynthesis is limited by incident light intensity and the availability of nutrients. Under ideal conditions very high growth rates can be achieved. Short term microalgal growth rates of 40 g m^{-2} d^{-1} (all rates are on a dry basis) and higher have been reported in experimental ponds (Tredici 2004). In well managed raceway ponds growth rates can be as high as 20 to 25 g m^{-2} d^{-1}, although values of 12 to 13 g m^{-2} d^{-1} are typical in the longer term for commercial raceway ponds. Corn growth rates over a crop rotation are about 13 g m^{-2} d^{-1}, although note that this is biomass above the soil; additional biomass grows below the soil. In all cases carbon content of the dry biomass is approximately 45 to 50%. These figures suggest that in perfect conditions incident solar radiation would support growth rates well above those noted in the case of *Dunaliella* in large unmixed ponds, which is about 1 g m^{-2} d^{-1}. This suggests that some nutrient must be limiting the growth in large unmixed ponds. Since carbon addition is required to sustain high growth rates in raceway ponds, we explore the rate of carbon flux into unmixed ponds.

4.4 Available Carbon

4.4.1 Ocean Water Carbon and pH

Ocean water contains approximately 28 milligrams of carbon per liter of water (Segar 1998). The dissolved inorganic carbon in ocean water is found mostly in four different species: aqueous carbon dioxide ($CO_2(aq)$), carbonic acid (H_2CO_3), bicarbonate (HCO_3^-), and carbonate (CO_3^{2-}). The amount of each species is determined by the pH of the solution and the pH of the solution is determined by the relative amount of each species. The bicarbonate-carbonate buffer is the most important buffer system for controlling pH and can provide carbon dioxide to the microalgae through the following reactions:

$$2HCO_3^- \Leftrightarrow CO_3^{2-} + H_2O + CO_2 \quad \text{(Eq. 4.4.1)}$$

$$HCO_3^- \Leftrightarrow CO_2 + OH^- \quad \text{(Eq. 4.4.2)}$$

$$CO_3^{2-} + H_2O \Leftrightarrow CO_2 + 2OH^- \quad \text{(Eq. 4.4.3)}$$

The pH of ocean water is approximately 8 at which the major inorganic carbon species is bicarbonate. As carbon dioxide is used by microalgae during photosynthesis, each of Equations 4.4.1 to 4.4.3 will shift to the right, forming hydroxide which increases the pH of the solution, assuming no other inorganic carbon is added to the solution. As the pH of the solution increases, carbonate becomes the dominant species which can then be converted to carbon dioxide (Eq. 4.4.3). The conversion of carbonate to carbon dioxide also further increases the pH of the solution.

The pH of the solution limits the amount of inorganic carbon that is available to the microalgae to use in photosynthesis. If all of the inorganic carbon in the ocean water based growth medium were converted to carbon dioxide (for use in photosynthesis) and hydroxide, the pH of the water would reach a value of about 14. The growth of most microalgal species becomes inhibited when the pH of the growth medium reaches a value of 10 to 11. For *Dunaliella*, growth is inhibited at a pH of 11 (Borowitzka and Borowitzka 1988), and hence not all of the inorganic carbon present in the medium is available to the microalgae for photosynthesis. For ocean water that starts at a pH of 8 and reaches a pH of 11, only about half of the initial total inorganic carbon is available for photosynthesis (Kaplan et al. 1986). Therefore in the absence of diffusion about 14 milligrams of carbon per liter of water are available to the microalgae for photosynthesis. For a pond depth of 0.2 m, this results in 2.8 grams of carbon per square meter of pond area being available for photosynthesis from the initial carbon content of the ocean water.

4.4.2 Carbon Flux

During growth in a pond additional carbon is supplied to the medium through gas exchange with the atmosphere. The flux of carbon dioxide from the atmosphere to water can be determined by the following formula (Wanninkhof 1992):

$$F = k(C_w - \alpha C_a) \qquad \text{(Eq. 4.4.4)}$$

Where:

F: carbon dioxide flux

k: gas transfer velocity

α: Ostwald solubility coefficient

C_w: CO_2 concentration in water

C_a: CO_2 concentration in air

The gas transfer velocity in Equation 4.4.4 represents the ease with which molecules of gas can transfer across the air-sea interface (Watson and Orr 2003) and is mostly dependent on wind speed. The gas transfer velocity was calculated using an empirical formula suggested by Wanninkhof (1992) and is mostly dependent on wind speed. The Ostwald solubility coefficient represents the ratio of the volume of gas (at standard temperature and pressure) absorbed by the liquid to the volume of the liquid and was calculated using an empirical formula suggested by Weiss (1974). For greater detail of Equation 4.4.4 and its use, see Appendix C.

Note that the carbon dioxide flux described in Equation 4.4.4 can also be increased due to hydration reactions of carbon dioxide (Equation 4.4.3) when the pH of the water is sufficiently high. However, this chemical enhancement of carbon dioxide flux is negligible at high gas transfer velocities and appears to be negligible at winds speeds of greater than 5 m s^{-1} (Wanninkhof 1992). For example, Wanninkhof and Knox (1996) report that the chemical enhancement of carbon dioxide flux only increases this flux by 5% for an average wind speed of 6 m s^{-1} at a location in the

equatorial Pacific. Given the high relative average wind velocity off the western coast of Australia of 5.4 m/s (see Table 2.3.1 above), the chemical enhancement of carbon dioxide flux is ignored in this work.

An alternative means for calculating carbon dioxide flux is given by Tans, Fung, and Takahashi (1990):

$$F = E\Delta pCO_2 \qquad \text{(Eq. 4.4.5)}$$

Where:

F: carbon dioxide flux

E: gas transfer coefficient

ΔpCO_2: partial pressure difference of CO_2 between water and air

The gas transfer coefficient in Equation 4.4.5 is the product of gas transfer velocity and solubility of carbon dioxide in seawater and is given as function of wind speed. For greater detail of Equation 4.4.5 and its use, see Appendix C.

The carbon dioxide concentration in an unmixed pond used for growing microalgae is not known: the microalgae are using available carbon up to the pH limit of 11. To determine an upper limit on carbon flux, it was calculate at a pond water concentration of zero, using Equations 4.4.4 and 4.4.5 with the following parameters:

- atmospheric temperature: 30°C
- pond water temperature: 30°C
- pond water salinity: 42 PSU
- wind speed: 5.4 m s^{-1} (which corresponds to the annual average wind speed)
- concentration of carbon dioxide in the atmosphere: 379 ppm

Based on these parameters, carbon dioxide flux from the atmosphere to the pond water is calculated as 1.15 g m^{-2} d^{-1} (Equation 4.4.4) and 1.75 g m^{-2} d^{-1} (Equation 4.4.5), which corresponds to a carbon flux of 0.32 and 0.48 g m^{-2} d^{-1}, respectively (see Appendix C for details of the calculations). This result approximately corresponds to observed long term growth rates in unmixed ponds growing *Dunaliella* in Australia (as discussed in Section 2.2.2) of 1 g m^{-2} d^{-1} of dry biomass with a carbon content of approximately 50% by weight (Schlesinger 1991). These ponds appear to be limited by carbon flux from the atmosphere, despite being designed to maximize mixing in the pond from predominant wind directions (L. J. Borowitzka 1991).

4.4.3 Total Available Carbon

Based on the amount of initial carbon available from the ocean water and the carbon added to the growth medium from flux with the atmosphere, the growth pattern in unmixed ponds would therefore use up all of the available carbon from the initial charge of sea water, about 14 mg l^{-1}, and then fall to 0.5 g m^{-2} per day. For a pond of 0.2 m depth, the total carbon in the microalgae can be approximated as 2.8 g plus 0.5 g m^{-2} per pond day, assuming the initial drawdown of carbon is rapid and the diffusion rate from the atmosphere becomes the growth limiting step early in the growth cycle.

4.5 Summary

Sunlight has the capacity to convert carbon into biomass at a rate at least one order of magnitude higher than it diffuses into seawater. Evaporation of sea water can produce a brine dense enough to transport biomass into the deep ocean in an annual average of 5 to 14 days. Other required nutrients such as nitrogen, phosphorus, potassium and micronutrients can be added to sea water as the pond fills. Diffusion of carbon dioxide into sea water is the rate limiting step in growing microalgae in unmixed ponds of seawater.

Chapter 5

Economic Feasibility of Microalgal Atmospheric Carbon Dioxide Capture and Storage Systems

5.1 Economic Feasibility of the Total Discharge Disposal System

5.1.1 Pond Area Requirements

As discussed in Section 2.4.3, discharge of the total unmixed pond water to the deep ocean would likely be done by pipeline rather than ship. The pipeline disposal system that directly connects the microalgal growth pond onshore to the deep ocean disposes virtually all of the culture water and microalgae in the growth pond into the deep ocean without processing it in any way. Therefore, all of the carbon that was taken up by the microalgae along with the carbon depleted culture medium is sent to the deep ocean. For a cycle time of 12 days, for example, microalgae in the discharge stream would contain approximately 8.8 g of carbon m^{-2} of pond surface; at a depth of 0.2 m, the microalgae would contain 44 g of carbon m^{-3} of discharge. However, only 6 g m^{-2} of surface (30 g of carbon m^{-3} of discharge) would come from the atmosphere; the remainder comes from drawing down the carbon that was initially in the sea water. Total carbon in the discharge stream would be 14 g of carbon from unconverted carbon in the initial sea water charge plus 44 g of carbon from the microalgae m^{-3} of discharge.

Since the purpose of operating a microalgal pond system is the transfer of carbon out of the atmosphere into the deep ocean, a reasonable approximation of the net flux from atmosphere to deep ocean for ponds with a total discharge to the deep ocean is 0.5 g m^{-2} d^{-1}, governed, as noted above, by the diffusion of carbon dioxide into unmixed sea water

The areal requirement for an unmixed microalgal pond with a depth of 0.2 m is therefore 1,494 m^2 t^{-1} yr^{-1} of carbon dioxide sequestered from the atmosphere (5480

$m^2\ t^{-1}\ yr^{-1}$ of carbon sequestered from the atmosphere). The low diffusivity of carbon dioxide translates into a very large areal requirement.

Each year, approximatley 4.1 Gt of carbon (15.0 Gt CO_2) is released into and remains in the atmosphere from the burning of fossil fuels (Solomon et al. 2007). If the total discharge disposal system were designed to transport all of this anthropogenic carbon into the deep ocean, the pond area required to capture this carbon would be 2.2×10^7 km^2 or 4700 km by 4700 km. This area is approximately 2.2 times greater than the area of Canada. It is highly unlikely that such a large area would be used for carbon sequestration.

5.1.2 Cost of the Microalgal Pond System using the Total Discharge Disposal System

A microalgal pond system based on total discharge would have a first cost based on land acquisition, permitting, construction of the pond system, sea water inlet, pumping water to the pond and power recovery from the discharge, nutrient receiving, storage and addition, pond water outlet, pipeline to the deep ocean for disposal of total pond water, plus related infrastructure (e.g. roads, docks, administration and maintenance buildings, etc.). Some additional investment would be required for a brine pond to spike discharge water during winter months of low evaporation. Operating cost would include pond and watercourse maintenance.

Given the large areal requirement, we first test the cost of carbon sequestration for a total discharge system by estimating the cost of the ponds alone. Wagener (1983) estimates the cost of pond construction at \$4 US m^{-2} of pond area. Assuming only this cost, a very long project life of 50 years, and a discount rate of 6% (appropriate for a social project, and low by conventional investment standards), the corresponding capital recovery factor is 0.063 and the cost of sequestering 1 tonne of carbon dioxide is \$379.

As was also noted in Section 2.4.2, a previous study sets a benchmark cost for capture of CO_2 from coal fired power plants located near tidewater (a port with shipping access to the ocean) and disposal into the deep ocean at \$90 to \$180 t^{-1} CO_2. Based on an estimated cost of pond construction alone with no consideration of water disposal costs, the cost of carbon capture via an unmixed microalgal pond is more than twice this value.

Therefore, because of the high areal requirements that in turn give a high capital cost, the microalgal atmospheric carbon dioxide capture and storage system using a pipeline disposal system is not feasible.

5.2 Economic Feasibility of the Microalgal Concentration Disposal System

5.2.1 Pond Area Requirements

In theory one could discharge a concentrated stream of microalgae via ship transport to a vertical pipe system (discussed in Section 2.4.4) or via a small dedicated pipeline. As will be shown below, the volume of water containing concentrated microalgae is very small compared to the total flow of ocean water, so in this section we consider ship based disposal through a suspended vertical pipe disposal system. This requires two separate discharge streams since the microalgae biomass is concentrated before it is disposed in to the deep ocean. The first discharge stream is the microalgae biomass concentrated by centrifuge which is transported by ship then pumped by density down a suspended vertical pipe to the deep ocean. The second discharge stream is the supernatant which is returned to the ocean surface. The supernatant discharge stream contains approximately 14 g m^{-3} of carbon or about half of that of the ocean surface water. Since the water being returned to the ocean surface contains less carbon than natural ocean water, this carbon depleted stream will drawn down carbon from the atmosphere until it equilibrates, reaching

the same carbon content as the original sea water, i.e. it will take up an additional 14 g m^{-3} of carbon from the atmosphere.

For a pond depth of 0.2 m and a one day cycle (i.e. the ponds are filled and emptied once every day, and ignoring for the moment the time to fill and drain the pond), a maximum of 3.3 g m^{-2} of carbon are available for microalgal growth with 2.8 g m^{-2} coming from the carbon in the initial ocean water and 0.5 g m^{-2} coming from diffusion from the atmosphere. Assuming that the microalgae is 50% carbon by weight, then the concentration of microalgae in the growth pond at the end of 1 day is approximately 0.0032% dry weight (DW). If nozzle centrifuges are used to concentrate the microalgae biomass, then the microalgal discharge stream can be concentrated to a dry weight content of up to 15% (Mohn 1988). If a concentration of only 1% DW is assumed for the microalgae biomass stream, then approximately 99.7% of the pond water is discharged as carbon depleted water to the ocean surface. This results in 3.3 g of carbon m^{-2} of pond area moving to the deep ocean, with 0.5 g coming from transfer from the atmosphere during the one day operating cycle and 2.8 g coming from drawdown of the carbon in the initial sea water charge, which is replenished by drawdown from the atmosphere after the supernatant discharge water is returned to the surface ocean. Care would have to be taken to prevent mixing between pond discharge and inlet water to insure maximum carbon uptake. Relative to the total discharge case, the concentrated microalgal case increases the rate of carbon uptake from approximately 0.5 to 3.3 g of carbon m^{-2} day^{-1}. The water discharged to the deep ocean is less than 0.5% of the total ocean water flowing through the system, assuming a microalgal concentration to 1% DW, an easily achieved target for *Dunaliella*.

The areal requirement for an unmixed microalgal pond with a depth of 0.2 m that operates on a one day cycle and uses a suspended vertical pipe system for disposal into the deep ocean is therefore 227 m^2 t^{-1} yr^{-1} of carbon dioxide sequestered from the atmosphere (832 m^2 t^{-1} yr^{-1} of carbon sequestered from the atmosphere).

If the microalgal concentration disposal system were designed to transport all of the anthropogenic carbon emissions from one year that remained in the atmosphere, 4.1 Gt of carbon (15.0 Gt CO_2) (Solomon et al. 2007), into the deep ocean, the pond area required to capture this carbon would be 3.4×10^6 km^2 or 1850 km by 1850 km. This area is equivalent to about one third of the area of Canada. Like the total discharge disposal system, it is highly unlikely that such a large area would be used for carbon sequestration.

5.2.2 Cost of the Microalgal Pond System using the Microalgal Concentration Disposal System

We take the same approach to cost as in Section 5.1.2: identify the cost of one or more major components of the system and do a screening test on the cost of carbon capture per tonne of carbon dioxide. Only if the economics are favourable at the preliminary screening would a more detailed cost analysis be warranted.

Using the same value for pond construction as in Section 5.1.2, \$4 m^{-2}, and the same project life of 50 years and discount rate of 6%, the carbon capture cost from the ponds alone is \$58 t^{-1} of carbon dioxide. However, both the capital and operating cost of centrifuges is high. Mohn (1988) reports a total cost of centrifuging m^{-3} of 0.72 Deutsche Marks (DM), equal to about \$0.48. At this value, the centrifuging cost per tonne of atmospheric carbon dioxide is more than \$6,500. Mohn's figures are based on 4800 operating hours per year, a discount rate of 10% and an amortization period of 5 years. If one takes Mohn's estimated capital cost of 170 kDM for 15 m^3 hr^{-1}, equivalent to \$94,550, and applies the capital recovery factor associated with a 50 year life and 6% discount rate, ignoring operating cost, the centrifuge cost is \$757 t^{-1} of carbon dioxide sequestered. Even if economy of scale and large scale purchasing could reduce the capital cost by a factor of 3, the cost of centrifuging is prohibitive relative to the alternative of direct capture from flue gas and disposal in the deep ocean. Note that Mohn identifies other methods of

microalgal separation, for example filtration, but costs are of the same order as for centrifugation.

The cost of centrifuging the microalgae could be reduced if the cycle time of the pond were increased or the depth of the pond decreased since for both cases the final density of the microalgae increases, that is more microalgae is processed through the centrifuge per volume of water. However, neither option can practically reduce the cost of concentrating the microalgae to a level that would make the system economically feasible. For example, in order for the cost of centrifuging the microalgae to be $100 per tonne of atmospheric carbon dioxide sequestered, the cycle time of the pond would have to be over one year. A retention time this long is not practical since microalgae would die over the course of the retention time period through predation and natural causes, and the carbon dioxide they captured would be released to the atmosphere. Also, the rate at which carbon dioxide that is sequestered from the atmosphere decreases as the cycle time of the pond increases. If the pond depth were decreased from 0.2 m to 0.1 m in order to increase the density of the microalgae the cost per tonne of atmospheric carbon dioxide sequestered would only decrease from $6,500 to $5,750. This cost is still too great to make centrifuging the microalgae feasible and in addition a consistent depth of 0.1 m is likely not practical for a large unmixed pond.

In essence, concentrating the microalgae is not feasible since the density of microalgae cell biomass in the pond water is so small; huge volumes of water need to be processed through the centrifuge in order to obtain a small amount of concentrated biomass. The ultimate cause of this is again the low rate of diffusion of carbon dioxide from the atmosphere to sea water. Because of the large volume of water compared to the small amount of biomass obtained, the cost of concentrating the microalgae is too high which renders the microalgal atmospheric carbon dioxide capture and storage system using a suspended vertical pipe disposal system unfeasible.

5.3 Summary

The total discharge of microalgal pond water through a pipeline into the deep ocean is limited as a means of capturing atmospheric carbon by the low rate of diffusion of carbon dioxide from the atmosphere, which is more than an order of magnitude lower than the rate at which sunlight can create biomass through photosynthesis. The low rate of carbon dioxide diffusion translates to a very high requirement for pond area, and the cost of pond area is simply too high to make microalgal growth a cost effective means of carbon capture relative to other alternatives.

Separation of microalgae from water allows a six fold increase in the net flux of carbon from the atmosphere because half the carbon in the original sea water is converted to biomass and disposed of in the deep ocean, in addition to the amount that diffuses into the pond. The highest net flux is realized with a short operating cycle, assumed to be one day in this study. The higher net carbon flux leads to a lower pond cost per tonne of carbon dioxide, but this is more than offset by the cost of microalgal separation: all methods of concentrating microalgae give a total cost of carbon sequestration that is higher than the alternative of direct capture from flue gas.

Chapter 6

Conclusion and Recommendations for Future Research

6.1 Conclusion

As more studies and modeling of the effects of greenhouse gas emissions on climate change are performed, an increasing number of methods for reducing the level of greenhouse gas in the atmosphere are being investigated. A method for directly capturing atmospheric carbon dioxide using photosynthesis and storing the carbon in the deep ocean was considered in this thesis. This method considered growing microalgae in large unmixed ponds and disposing the microalgal biomass in the deep ocean. Two disposal concepts were considered, discharging all of the pond culture medium and discharging a concentrated stream of microalgae after concentrating the biomass.

The transfer of carbon dioxide from the atmosphere to large unmixed ponds is the rate limiting process in the growth of microalgae when no additional carbon is added to the growth medium. Because the diffusion of carbon dioxide from the atmosphere to pond water is low, approximately 0.5 g of carbon d^{-1} m^{-2} of pond area, the growth rate per area is also low, approximately 1 g of biomass d^{-1} m^{-2} of pond area, which then requires a large pond surface area in order to grow a significant amount of microalgal biomass.

For an atmospheric carbon dioxide capture and storage system that disposes microalgae biomass into the deep ocean, the large area requirement results in a low density of microalgae cell biomass in the pond water. The low microalgae cell biomass densities result in the cost of the carbon dioxide capture and storage system being significantly higher than other carbon dioxide sequestration methods. One benchmark test for carbon sequestration schemes is the estimated cost of

sequestering carbon dioxide from flue gas from coal fired power plants, estimated at $90 to $180 per tonne of carbon dioxide for power plants located near tidewater (Fujioka et al. 1997).

For the system where the microalgae is discharged to the deep ocean with all of the growth medium, the area requirement, approximately 5,500 m^2 t^{-1} of carbon sequestered y^{-1}, is sufficiently high that the construction cost per tonne of carbon dioxide sequestered per year of the microalgae growth pond, approximately $400, renders the system unfeasible. For the system where the microalgae is first concentrated then discharged to the deep ocean and the supernatant is returned to the ocean surface the capital recovery cost from the high investment in equipment for concentrating the microalgae, approximately $750 t^{-1} CO_2 sequestered, renders the system unfeasible even before considering the cost of operating the centrifuges, e.g. power and maintenance. Ultimately, the cost of sequestering atmospheric carbon dioxide by growing microalgae in unmixed ponds and disposing it in the deep ocean is too high because of the low diffusion of carbon dioxide from the atmosphere to the pond water which results in low microalgae densities.

6.2 Recommendations for Future Research

The cost of carbon sequestration for growth of biomass in seawater is so high relative to benchmark alternatives that no further research is recommended. Microalgal growth plants have very high value products, e.g. high value food products, and many enhance the rate of carbon dioxide transfer by mixing and carbon addition. Research and development is underway to capture carbon dioxide from significantly enhanced gas streams, e.g. flue gas, to produce a valuable product such as biodiesel (see, for example, Keffer and Kleinheinz 2002; Chisti 2007). However, using microalgal growth purely to sequester carbon from the atmosphere is not economic compared to carbon sequestration from flue gas.

The growth rate of biomass on land is more than an order of magnitude higher than the diffusion rate of carbon dioxide into seawater because the barrier of diffusion from atmosphere to water is avoided. Hence one might conceive of a process involving growing land based biomass and sinking it into the deep ocean. Two factors militate against this alternative. First, most land based biomass is significantly less dense than sea water, which means that either a long soaking process or a weighting scheme would be required. In addition, once land based biomass is accumulated it has a more valuable alternative than simple sequestration: it can be used as an energy source for electricity or biofuel production, for example, displacing fossil fuel that would otherwise be required.

Other forms of direct capture of carbon dioxide from the atmosphere are possible, e.g. adsorption on zeolites or absorption in liquids such as mono or diethanol amine. Given the relatively low concentration of carbon dioxide in the atmosphere, these methods would require careful cost screening. One can note that plants have evolved over hundreds of millions of years to efficiently capture carbon dioxide from the atmosphere at low concentrations. Hence the use of terrestrial plant biomass as an energy source may be the most effective means of abating the impact of fossil fuel usage, by displacement of future emissions rather than removal of current carbon dioxide from the atmosphere.

References

Avery, W. H., and C. Wu. 1994. *Renewable energy from the ocean: A guide to OTEC*. New York: Oxford University Press.

Barsanti, L., and P. Gualtieri. 2006. *Algae: Anatomy, biochemistry, and biotechnology*. Boca Raton, FL: CRC Press.

Becker, W. 2004. Microalgae in human and animal nutrition. In *Handbook of microalgal culture: Biotechnology and applied phycology*, ed. A. Richmond, 312-351. Oxford: Blackwell Science.

Ben-Amotz, A. 2004. Industrial production of microalgal cell-mass and secondary products- major industrial species: *Dunaliella*. In *Handbook of microalgal culture: Biotechnology and applied phycology*, ed. A. Richmond, 273-280. Oxford: Blackwell Science.

Bender, W. J., A. N. Blair, and B. M. Ayyub. 2001. US industrial capacity and risk-based simulation for the construction of the mobile offshore base. *Proceedings of OMAE '01 20th international conference on offshore mechanics and arctic engineering*. Rio de Janeiro, June 2001.

Blanco-Canqui, H., R. Lal, W. M. Post, and L. B. Owens. 2006. Changes in long-term no-till corn growth and yield under different rates of stover mulch. *Agronomy journal* 98:1128-1136, http://www.scopus.com (accessed March 9, 2007).

Bindoff, N.L., J. Willebrand, V. Artale, A, Cazenave, J. Gregory, S. Gulev, K. Hanawa et al. 2007. Observations: Oceanic climate change and sea level. In *Climate change 2007: The Physical Science Basis,* eds. S. Solomon, D. Qin, M.

Manning, Z. Chen, M. Marquis, K.B. Averyt, M. Tignor, and H.L. Miller, 385-432. New York: Cambridge University Press. http://www.ipcc.ch/ipccreports/ar4-wg1.htm (accessed September 10, 2007).

Borowitzka, L. J. 1991. Development of Western Biotechnology's algal β-carotene plant. *Bioresource technology* 38:251-252, http://www.scopus.com (accessed March 8, 2007).

Borowitzka, M. A. 1990. The mass culture of *Dunaliella salina. Technical resource papers regional workshop on the culture and utilization of seaweeds volume II.* Cebu City, Philippines. http://www.fao.org/docrep/field/003/AB728E/AB728E06.htm#ch6 (accessed October 16, 2007).

Borowitzka, M. A., and L. J. Borowitzka. (1988). *Dunaliella*. In *Micro-algal biotechnology*, eds. M. A. Borowitzka, and L. J. Borowitzka, 27-58. Cambridge: Cambridge University Press.

Caldeira, K., M. Akai, P. Brewer, B. Chen, P. Haugan, T. Iwama, P. Johnston et al. 2005. Ocean Storage. In *IPCC Special Report on Carbon Dioxide Capture and Storage*, eds. B. Metz, O. Davidson, H. de Coninck, M. Loos, and L. Meyer, 277-318. New York: Cambridge University Press.

Chakrabarti, S. K. 2005. *Handbook of Offshore Engineering*. vol. 2. Oxford: Elsevier. http://www.knovel.com/knovel2/Toc.jsp?BookID=1660&VerticalID=0 (accessed December 3, 2007).

Chisti, Y. 2007. Biodiesel from microalgae. *Biotechnology advances* 25:294-306, http://www.scopus.com (accessed February 8, 2008).

COA. *See* Commonwealth of Australia.

Commonwealth of Australia, Bureau of Meteorology. 2007. *Climate statistics for Australian locations*. http://www.bom.gov.au/climate/averages/tables/cw_008051_All.shtml (accessed November 7, 2007).

Dodd, J. C. 1986. Elements of pond design and construction. In *Handbook of microalgal mass culture,* ed. A. Richmond, 265-284. Boca Raton, FL: CRC Press.

Doney, S. C., K. Lindsay, and J. K. Moore. 2003. Global ocean carbon cycle modeling. In *Ocean biogeochemistry: The role of the ocean carbon cycle in global change*, ed. M. J. R. Fasham, 217-238. Springer-Verlag: Berlin.

Figueiredo C., P.C. Flynn, and E. A. Cabral. 2006. The economics of energy storage in 14 deregulated power markets. *Energy Studies Review* 14(2):131-152.

Fujioka, Y., M. Ozaki, K. Takeuchi, Y. Shindo, and H. J. Herzog. 1997. Cost comparison in various CO_2 ocean disposal options. *Energy conversion management* 38:S273-S277, http://www.scopus.com (accessed May 17, 2007).

Haaland, S. E. 1983. Simple and explicit formulas for the friction factor in turbulent pipe flow. *Journal of fluids engineering* 105 (March):89-90.

Hu, Q. 2004. Industrial production of microalgal cell-mass and secondary products-major industrial species: *Arthrospira* (*Spirulina*) *platensis*. In *Handbook of microalgal culture: Biotechnology and applied phycology*, ed. A. Richmond, 264-272. Oxford: Blackwell Science.

Iwamoto, H. 2004. Industrial production of microalgal cell-mass and secondary products- major industrial species: *Chlorella*. In *Handbook of microalgal culture: Biotechnology and applied phycology*, ed. A. Richmond, 255-263. Oxford: Blackwell Science.

Jahne, B., G. Heinz, and W. Dietrich. 1987. Measurement of the diffusion coefficients of sparingly soluble gases in water with a modified Barrer method. *Journal of geophysical research* 92 (10):10,767-10,776

Kaplan, D., A. E. Richmond, Z. Dubinsky, and S. Aaronson. 1986. Algal nutrition. In *Handbook of microalgal mass culture,* ed. A. Richmond, 265-284. Boca Raton, FL: CRC Press.

Keffer, J. E., and G. T. Kleinheinz. 2002. Use of *Chlorella vulgaris* for CO_2 mitigation in a photobioreactor. *Journal of industrial microbiology & biotechnology* 29:275-280, http://www.scopus.com (accessed September 26, 2006).

Lee, R. E. 1989. *Phycology*. 2nd ed. Cambridge: Cambridge University Press.

Lee, Y. K. 1997. Commercial production of microalgae in the Asia-Pacific rim. *Journal of applied phycology* 9:403-411, http://www.scopus.com (accessed November 27, 2006).

Lee, Y. K. 2001. Microalgal mass culture systems and methods: Their limitations and potential. *Journal of applied phycology* 13:307-315, http://www.scopus.com (accessed March 6, 2007).

Li, Y., and P.C. Flynn. 2003. Power prices in deregulated markets. *2003 IEEE Power Engineering Society general meeting, conference proceedings* 2:874-879.

Makai Ocean Engineering Inc. 2007. Deep Pipelines for Aquaculture. http://www.makai.com/p-aquaculture.htm (accessed November 27, 2007).

Marshall J., and F. Schott. 1999. Open-ocean convection: Observations, theory, and models. *Reviews of geophysics* 37 (1):1-64, http://www.scopus.com (accessed November 21, 2006).

Masojidek, J., M. Koblizek, and G. Torzillo. 2004. Photosynthesis in Microalgae. In *Handbook of microalgal culture: Biotechnology and applied phycology*, ed. A. Richmond, 20-39. Oxford: Blackwell Science.

Meehl, G. A., T. F. Stocker, W. D. Collins, P. Friedlingstein, A. T. Gaye, J. M. Gregory, A. Kitoh, et al. 2007. Global Climate Projections. In *Climate change 2007: The physical science basis,* eds. S. Solomon, D. Qin, M. Manning, Z. Chen, M. Marquis, K.B. Averyt, M. Tignor, and H.L. Miller, 747-845. New York: Cambridge University Press. http://www.ipcc.ch/ipccreports/ar4-wg1.htm (accessed September 6, 2007).

Millero, F. J., and A. Poisson. 1981. International one-atmosphere equation of state of seawater. *Deep-sea research* 28A (6):625-629, http://www.scopus.com (accessed September 21, 2006).

Mohn, F. H. 1988. Harvesting of micro-algal biomass. In *Micro-algal biotechnology*, eds. M. A. Borowitzka, and L. J. Borowitzka, 395-414. Cambridge: Cambridge University Press.

Mott, R.L. 2006. *Applied fluid mechanics*. 6th ed. Upper Saddle River, NJ: Pearson Prentice Hall.

Nakada, S., and H. Suzuki. 2004. Optimization of the dynamic response of a semi-submersible type Megafloat. *Ocean '04- MTS/IEEE Techno-Ocean '04: Bridge across the ocean- conference proceedings* 2:1073-1079.

National Oceanography Centre. 2008. *Ocean Observing and Climate*. http://www.noc.soton.ac.uk/ooc/CLIMATOLOGY/noc1_1.php (accessed February 1, 2008).

NOC. *See* National Oceanography Centre.

Oswald, W. J. 1988. Large-scale algal culture systems (engineering aspects). In *Micro-algal biotechnology*, eds. M. A. Borowitzka, and L. J. Borowitzka, 357-394. Cambridge: Cambridge University Press.

Poisson, A., and M. H. Gadhoumi. 1993. An extension of the Practical Salinity Scale 1978 and the Equation of State 1980 to high salinities. *Deep-sea researche I* 40 (8):1689-1698.

Richmond, A. 1986. Outdoor mass Cultures of microalgae. In *Handbook of microalgal mass culture,* ed. A. Richmond, 285-330. Boca Raton, FL: CRC Press.

Schlesinger, W. H. 1991. *Biogeochemistry: An analysis of global change*. San Diego: Academic Press.

Segar, D. A. 1998. *Introduction to ocean sciences*. Belmont, CA: Wadsworth Publishing.

Solomon, S., D. Qin, M. Manning, R.B. Alley, T. Berntsen, N.L. Bindoff, Z. Chen et al. 2007. Technical summary. In *Climate change 2007: The physical science basis,* eds. S. Solomon, D. Qin, M. Manning, Z. Chen, M. Marquis, K.B. Averyt,

M. Tignor, and H.L. Miller, 19-91. New York: Cambridge University Press. http://www.ipcc.ch/ipccreports/ar4-wg1.htm (accessed September 6, 2007).

Spolaore, P., C. Joannis-Cassan, E. Duran, and A. Isambert. 2006. Commercial application of microalgae. *Journal of bioscience and bioengineering* 101 (2):87-96, http://www.scopus.com (accessed November 27, 2006).

Stern, K. R., S. Jansky, and J. E. Bidlack. 2003. *Introductory plant biology*. 9th ed. New York: McGraw- Hill.

Tans, P. P., I. Y. Fung, and T. Takahashi. 1990. Observational constraints on the global atmoshpheric CO_2 budget. *Science* 247 (4949):1431-1438, http://www.scopus.com (accessed January 16, 2008).

Tomaselli, L. 2004. The microalgal cell. In *Handbook of microalgal culture: Biotechnology and applied phycology*, ed. A. Richmond, 20-39. Oxford: Blackwell Science.

Tredici, M. R. 2004. Mass production of microalgae: Photobioreactors. In *Handbook of microalgal culture: Biotechnology and applied phycology*, ed. A. Richmond, 178-214. Oxford: Blackwell Science.

Treguer, P., L. Legendre, R. T. Rivkin, O. Regueneau, and N. Dittert. 2003. In *Ocean biogeochemistry: The role of the ocean carbon cycle in global change*, ed. M. J. R. Fasham, 145-156. Springer-Verlag: Berlin.

Trenberth, K. E., P. D. Jones, P. Ambenje, R. Bojariu, D. Easterling, A. Klein Tank, D. Parker et al. 2007. Observations: Surface and Atmospheric Climate Change. In *Climate change 2007: The physical science basis,* eds. S. Solomon, D. Qin, M. Manning, Z. Chen, M. Marquis, K.B. Averyt, M. Tignor, and H.L. Miller,

235-336. New York: Cambridge University Press. http://www.ipcc.ch/ipccreports/ar4-wg1.htm (accessed September 7, 2007).

Turner, J. T. 2002. Zooplankton fecal pellets, marine snow and sinking phytoplankton blooms. *Aquatic microbial ecology* 27:57-102, http://www.scopus.com (accessed January 10, 2007).

U.S. Department of Commerce, National Oceanic and Atmospheric Administration, National Geophysical Data Center. 2006. *2-minute Gridded Global Relief Data (ETOPO2v2)*. http://www.ngdc.noaa.gov/mgg/fliers/06mgg01.html (accessed December 13, 2006).

U.S. Department of Commerce, National Oceanic and Atmospheric Administration, National Oceanographic Data Center. 2007. *Access Argo Data*. http://www.nodc.noaa.gov/argo/accessData.htm (accessed December 6, 2007).

USDOC. *See* U.S. Department of Commerce.

Wagener, K. 1983. Mass cultures of marine algae for energy farming in coastal deserts. *International journal of biometeorology* 27 (3):227-233, http://www.scopus.com (accessed September 25, 2007).

Wanninkhof, R. 1992. Relationship between wind speed and gas exchange over the ocean. *Journal of geophysical research* 97 (C5):7373-7382.

Wanninkhof, R., and M. Knox. 1996. Chemical enhancement of CO_2 exchange in natural waters. *Limnology and oceanography* 41 (4):689-697, http://www.scopus.com (accessed January 14, 2008).

Watanabe, E., T. Utsunomiya, and C. M. Wang. 2004. Hydroelastic analysis of pontoon-type VLFS: a literature survey. *Engineering Structures* 26 (2):245-256, http://www.scopus.com (accessed March 22, 2007).

Watson, A. J., J. C. Orr. 2003. Carbon dioxide fluxes in the global ocean. In *Ocean biogeochemistry: The role of the ocean carbon cycle in global change*, ed. M. J. R. Fasham, 123-143. Springer-Verlag: Berlin.

Weiss, R. F. 1974. Carbon dioxide in water and seawater: the solubility of a non-ideal gas. *Marine chemistry* 2:203-215, http://www.scopus.com (accessed July 10, 2007).

White, F. M. 2003. *Fluid Mechanics*. 5th ed. New York: McGraw-Hill.

Appendix A

The density of seawater can be calculated from temperatures ranging from 0 to 40°C and salinities ranging from 0.5 to 43 PSU using the international one-atmosphere equation of state of seawater (Millero and Poisson 1981) which is given as follows:

$$\rho = \rho_0 + AS + BS^{3/2} + CS^2 \qquad \text{(Eq. A1)}$$

$$\rho_0 = D_0 + D_1 t + D_2 t^2 + D_3 t^3 + D_4 t^4 + D_5 t^5 \qquad \text{(Eq. A2)}$$

$$A = A_0 + A_1 t + A_2 t^2 + A_3 t^3 + A_4 t^4 \qquad \text{(Eq. A3)}$$

$$B = B_0 + B_1 t + B_2 t^2 \qquad \text{(Eq. A4)}$$

$$C = C_0 \qquad \text{(Eq. A5)}$$

Where:

ρ: density of seawater (kg m^{-3})

ρ_0: density of pure water (kg m^{-3})

S: salinity (PSU)

t: temperature (°C)

The coefficients (A, B, C, and D) in Equations A2 to A5 are given in Table A1.

Table A1: Values of the coefficients in Equations A2 to A5.

Coefficient	Value	Coefficient	Value
A_0	8.24493×10^{-1}	C_0	4.8314×10^{-4}
A_1	-4.0899×10^{-3}		
A_2	7.6438×10^{-5}	D_0	9.99842594×10^{2}
A_3	-8.2467×10^{-7}	D_1	6.793952×10^{-2}
A_4	5.3875×10^{-9}	D_2	-9.095290×10^{-3}
		D_3	1.001685×10^{-4}
B_0	-5.72466×10^{-3}	D_4	1.120083×10^{-6}
B_1	1.0227×10^{-4}	D_5	6.536332×10^{-9}
B_2	-1.6546×10^{-6}		

Poisson and Gadhoumi (1993) extend the equation of state for salinities from 42 to 50 PSU for temperatures ranging from 10 to 30°C which is given as follows:

$$\rho = \rho_0 + S\left(A_0 + A_1 t + A_2 S + A_3 t^2 + A_4 tS + A_5 S^2 + A_6 t^3 + A_7 t^2 S + A_8 tS^2 + A_9 S^3\right)$$

(Eq. A6)

Where:

ρ: density of seawater (kg m^{-3})

ρ_0: density of pure water (kg m^{-3})

S: salinity (PSU)

t: temperature (°C)

The density of pure water, ρ_0, given by Equation A2 and the coefficients in Equation A6 are given in Table A2.

Table A2: Values of the coefficients in Equation A6.

Coefficient	Value	Coefficient	Value
A_0	82.4427×10^{-2}	A_5	-14.791×10^{-6}
A_1	-52.753×10^{-4}	A_6	67.90×10^{-8}
A_2	-51.17×10^{-5}	A_7	-15.886×10^{-7}
A_3	40.261×10^{-6}	A_8	-52.228×10^{-8}
A_4	11.5114×10^{-5}	A_9	20.750×10^{-8}

Appendix B

The following MATLAB code, pipe.m and dens0.m, was used to calculate the density of the pond water required to produce flow in the down flow pipe.

pipe.m

```
function pipe

depth = xlsread('5900785.xls',1, 'C2:C117'); %outside density profile depth
(m)
rhoo = dens_pro;   %outside density profile

zd = 800;      %(m) disposal depth
hd = 95e3;        %(m) distance covered by pipeline

i = 1;
while depth(i) <= zd

   z0p(i) = depth(i);   %depth profile from 0 to z2
   i=i+1;
end

m = length(z0p);

z2 = z0p(m);    %depth at z2

for j=1:m

   rhoo0(j) = rhoo(j);  % density profile outside the pipe from 0 to z2
end

for j=2:m

   I0i(j) = (z0p(j)-z0p(j-1))*0.5*(rhoo0(j-1)+rhoo0(j));
         %piecewise numerical integration from 0 to 2
end

I0 = sum(I0i);  %sum of integration from 0 to 2

z1 = 1;       %Assume z1 (m)

i=1;
j=1;
k=1;

L = (z2-z1) + hd;       %(m) length of pipe (vertical + horizontal distance)

while depth(i) < zd

   if depth(j) < z1

      z1pl(k) = depth(j);    %depth profile from <z1 to z2
      rhoo1l(k) = rhoo(j);   %%density profile from <z1 to z2
      k=k+1;
```

```
  else

    z1pg(i) = depth(j);     %depth profile from >z1 to z2
    rhoo1g(i) = rhoo(j);    %density profile from >z1 to z2
    i=i+1;
  end

  j=j+1;
end

z1p = [z1, z1pg];      %density profile from z1 to z2

m1l = length(z1pl);    %lenght of depth profile from <z1 to z2 matrix

rhoo1z1 = rhoo1l(m1l) + (z1-z1pl(m1l))/(rhoo1g(1)-z1pl(m1l))*(rhoo1g(1)-...
          rhoo1l(m1l));  %interpolate to find the density at z1

rhoo1 = [rhoo1z1, rhoo1g];     %density profile from z1 to z2

for k=2:m

I1i(k) = (z1p(k)-z1p(k-1))*0.5*(rhoo1(k-1)+rhoo1(k));
         %piecewise numerical integration from 1 to 2

end

I1 = sum(I1i);  %sum of integration from 1 to 2

g = 9.81;      %gravity (m/s^2)

%Pipe Characteristics
d = 7.5;       %diameter (m)
eta = 0.04e-3;  %roughness (m) -FRP

%Flow Characteristics
V = 1.5;       %fluid velocity (m/s)
mu = 1.07e-3;  %viscosity (kg/(m-s))

rhoi = 1000;  %initial guess of inside density


tolr = 1e-6;
diffr = 1;
countr = 0;


while tolr < diffr && countr < 1000

   Red = rhoi*V*d/mu;

   if Red < 4000

      f = 64/Red;
```

```
    else

       f = (-1.8*log((6.9/Red)+((eta/d)/3.7)^1.11))^-2;
    end

    hf = f*L/d*V^2/2/g;

    rhoi_new = (I0 + I1)/(2*z2 - 2*z1 - hf);

    diffr = abs(rhoi_new - rhoi);
    rhoi = rhoi_new;

    countr = 1 + countr;

  end

  fid = fopen('pipe.txt', 'w');
  fprintf(fid, 'Density of Water Inside the Pipe\n');
  fprintf(fid, '--------------------------------\n\n');
  fprintf(fid, 'Pipe Material:   concrete\n\n');
  fprintf(fid, 'Disposal Depth:      %6.1f m\n', z2);
  fprintf(fid, 'Horizontal Distance:  %6.1f m\n', hd);
  fprintf(fid, 'Water Level in Pipe:  %6.2f m\n', z1);
  fprintf(fid, 'Pipe Length:         %6.1f m\n\n', L);
  fprintf(fid, 'Pipe Diameter:       %6.2f m\n', d);
  fprintf(fid, 'Pipe Roughness:    %6.2e m\n', eta);
  fprintf(fid, 'Flow Velocity:       %6.2f m/s\n', V);
  fprintf(fid, '\nDensity:           %6.2f kg/m^3 \n', rhoi);
  fclose(fid);

  fprintf('rho = %6.4f\n', rhoi)
```

dens0.m

```
function rho = dens0(S,T)

%Valid for 0<T<40 and 0.5<S<43

%Density of Standard Mean Ocean Water
D0 = 999.842594;
D1 = 6.793952e-02;
D2 = -9.095290e-03;
D3 = 1.001685e-04;
D4 = -1.120083e-06;
D5 = 6.536332e-09;

D = D0 + D1*T + D2*T^2 + D3*T^3 + D4*T^4 + D5*T^5;

if S >=0.5 && S <43

 %Coefficients
A0 = 8.24493e-01;
```

```
        A1 = -4.0899e-03;
        A2 = 7.6438e-05;
        A3 = -8.2467e-07;
        A4 = 5.3875e-09;

        B0 = -5.72466e-03;
        B1 = 1.0227e-04;
        B2 = -1.6546e-06;

        C0 = 4.8314e-04;

        A = A0 + A1*T + A2*T^2 + A3*T^3 + A4*T^4;
        B = B0 + B1*T + B2*T^2;
        C = C0;

        rho = D + A*S + B*S^(3/2) +C*S^2;

        elseif S >= 43 && S <= 50

        A0 = 82.4427e-2;
        A1 = -52.753e-4;
        A2 = -51.17e-5;
        A3 = 40.261e-6;
        A4 = 11.5114e-5;
        A5 = -14.791e-6;
        A6 = 67.90e-8;
        A7 = -15.886e-7;
        A8 = -52.228e-8;
        A9 = 20.750e-8;

        rho = D + S*(A0 + A1*T + A2*S +A3*T^2 + A4*T*S + A5*S^2 + A6*T^3 +
        A7*T^2*S...
                + A8*T*S^2 + A9*S^3);

else

   disp('Salinity must be 0.5 <= S <= 50')
end
```

Appendix C

The exchange of carbon dioxide from the atmosphere to the pond water was calculated using the methods described by Wanninkhof (1992) and Tans, Fung, and Takahashi (1990).

Wanninkhof

Table C1: List of symbols used to calculate CO_2 flux using the method described by Wanninkhof.

Symbol	Description	Units
α	Ostwald solubility coefficient	$m^3\ m^{-3}$
C_a	gas concentration in air	$m^3\ m^{-3}$
C_w	gas concentration in water	$m^3\ m^{-3}$
F	flux	$m\ s^{-1}$
F_m	mass flux	$kg\ m^{-2}\ s^{-1}$
k	gas transfer velocity	$m\ s^{-1}$
K_o	solubility coefficient	$mol\ kg^{-1}\ atm^{-1}$
MW	molecular weight of gas	$g\ mol^{-1}$
p	pressure of gas	Pa
R	universal gas constant	$J\ K^{-1}\ mol^{-1}$
ρ_g	density of gas	$kg\ m^{-3}$
ρ_l	density of water	$kg\ m^{-3}$
S	salinity of water	ppt
Sc	Schmidt Number	-
T	absolute temperature	K
t	temperature	^oC
u	wind speed	$m\ s^{-1}$
v^+	molar volume of gas at STP	$m^3\ mol^{-1}$

$$F = k(C_w - \alpha C_a) \qquad \text{(Eq. C1)}$$

$$k = 0.31u^2\left(\frac{Sc}{660}\right)^{-1/2} \qquad \text{(Eq. C2)}$$

$$Sc = D_0 - D_1 t + D_2 t^2 - D_3 t^3 \qquad \text{(Eq. C3)}$$

$$\alpha = K_0 \rho_l v^+ \frac{T}{273.15} \qquad \text{(Eq. C4)}$$

$$\ln K_0 = A_1 + A_2\left(\frac{100}{T}\right) + A_3 \ln\left(\frac{T}{100}\right) + S\left[B_1 + B_2\left(\frac{T}{100}\right) + B_3\left(\frac{T}{100}\right)^2\right] \qquad \text{(Eq. C5)}$$

$$v^+ = \frac{RT}{p} \qquad \text{(Eq. C6)}$$

Equation C1 gives CO_2 flux in units of m s^{-1} or m^3 m^{-2} s^{-1}. To convert to mass flux (kg m^{-2} s^{-1}) F needs to be multiple by the density of carbon dioxide:

$$\rho_g = \frac{MW}{R}\frac{p}{T} \qquad \text{(Eq. C7)}$$

$$F_m = \rho_g F \qquad \text{(Eq. C8)}$$

Note that Equation C3 is given by Jahne, Heinz, and Dietrich (1987) and Equation C5 is given by Weiss (1974). The density of water, ρ_l, in Equation C4 can be found using the equation of state as described in Appendix A. The coefficients in Equation C3 are given in Table C2 and the coefficients in Equation C5 are given in Table C3. A summary of carbon dioxide flux calculations using this method is given in Table C4; note that a negative flux indicates transfer from the atmosphere to the water.

Table C2: Values of the coefficients in Equation C3.

Coefficient	Value
D_0	2073.1
D_1	125.62
D_2	3.6276
D_3	0.043219

Table C3: Values of the coefficients in Equation C5.

Coefficient	Value	Coefficient	Value
A_1	-60.2409	B_1	0.023517
A_2	93.4517	B_2	-0.23656
A_3	23.3585	B_3	0.0047036

Table C4: Input and output parameters used to calculate CO_2 flux as described by Wanninkhof.

Parameter	Value	Unit	Equation
Input			
temperature, t	30	°C	
absolute temperature, T	303.15	K	
pressure of gas, p	101,325	Pa	
universal gas constant, R	8.3124	$J\ K^{-1}\ mol^{-1}$	
salinity of water, S	42	ppt	
wind speed, u	5.5	$m\ s^{-1}$	
CO_2 concentration in water, C_w	0	$m^3\ m^{-3}$	
CO_2 concentration in air, C_a	379×10^{-6}	$m^3\ m^{-3}$	
molecular weight of CO_2 MW	44.0	$g\ mol^{-1}$	
Output			
molar volume of CO_2 at STP, v^+	0.0224	$m^3\ mol^{-1}$	C6
solubility coefficient, K_o	0.0243	$mol\ kg^{-1}\ atm^{-1}$	C5
density of water, ρ_l	1027.7	$kg\ m^{-3}$	*
Ostwald solubility coefficient, α	0.622	$m^3\ m^{-3}$	C4
Schmidt Number, Sc	402.4	-	C3
gas transfer velocity, k	3.22×10^{-5}	$m\ s^{-1}$	C2
CO_2 flux, F	-7.57×10^{-9}	$m\ s^{-1}$	C1
density of CO_2, ρ_g	1.77	$kg\ m^{-3}$	C7
CO_2 mass flux, F_m	-1.34×10^{-8}	$kg\ m^{-2}\ s^{-1}$	C8
CO_2 mass flux	-1.16	$g\ m^{-2}\ d^{-1}$	
C mass flux	-0.316	$g\ m^{-2}\ d^{-1}$	

*Equation of state, see Appendix A

Table C5: List of symbols used to calculate CO_2 flux using the method described by Tans, Fung, and Takahashi.

Symbol	Description	Units
E	gas transfer coefficient	mol m^{-2} yr^{-1} μatm^{-1}
F	flux	mol m^{-2} yr^{-1}
F_m	mass flux	g m^{-2} yr^{-1}
MW	molecular weight of gas	g mol^{-1}
ΔpCO_2	CO_2 partial pressure difference (air and water)	μatm
W	wind speed	m s^{-1}

$$F = E\Delta pCO_2 \qquad \text{(Eq. C9)}$$

$$E = \begin{cases} 0 & W < 3 \\ 0.016(W-3) & W \geq 3 \end{cases} \qquad \text{(Eq. C10)}$$

$$F_m = (MW)F \qquad \text{(Eq. C11)}$$

Table C6: Input and output parameters used to calculate CO_2 flux as described by Tans, Fung, and Takahashi.

Parameter	Value	Unit	Equation
Input			
wind speed, W	5.4	m s^{-1}	
CO_2 partial pressure difference, ΔpCO_2	379	μatm	
molecular weight of CO_2 MW	44.0	g mol^{-1}	
Output			
gas transfer coefficient, E	0.0384	mol m^{-2} yr^{-1} μatm^{-1}	C10
CO_2 flux, F	14.6	mol m^{-2} yr^{-1}	C9
CO_2 mass flux, F_m	640	g m^{-2} yr^{-1}	C11
CO_2 mass flux	1.75	g m^{-2} d^{-1}	
C mass flux	0.478	g m^{-2} d^{-1}	